Micro-additive manufacturing technologies of three-dimensional MEMS

Hassanin, H., Sheikholeslami, G., Pooya, S. and Ishaq, R.

Micro-Additive Manufacturing Technologies of Three-Dimensional MEMS

Hany Hassanin[1]*, Ghazal Sheikholeslami[1], Pooya Sareh[2], and Rihana B. Ishaq[1]

[1] School of Engineering, Technology, and Design, Canterbury Christ Church University, Canterbury, UK

[2] Creative Design Engineering Lab (Cdel), School of Engineering, University of Liverpool, Liverpool, L69 3GH, UK

[*] Corresponding author: Dr Hany Hassanin, Email: hany.hassanin@canterbury.ac.uk

Abstract

Conventional microfabrication processes have been well established, but their capabilities are generally limited simple and 2D extruded geometries. Additive manufacturing allows the ability to manufacture true 3D complex geometries, rapid design for manufacturing, mass customisation, materials savings, and high precision which have triggered the increased interest in manufacturing microelectromechanical systems (MEMS). This paper consolidates MEMS manufacturing's recent advancements, including both conventional and additive manufacturing technologies, their working principles, and practical capabilities. The paper also discusses in detail the use of additive manufacturing in several MEMS areas such as in microelectronics, circuitry, microfluidics, lab on a chip, packaging, and structural MEMS. Furthermore, the potentials and limitations of additive manufacturing are investigated with regards to the MEMS requirements. Finally, the technology outlook and improvements are discussed. This study showed that additive manufacturing has offered a promising future for the fabrication of microelectromechanical systems, especially using high resolution techniques such as microstereolithography, materials jetting, and materials extrusion. On the other hand, current challenges such as materials requirements, equipment innovation, fabricating of in vivo devices for biomedical applications, inherited defects and poor surface finish, adhesion to substrates, and productivity are areas that requires further study to increase the uptake by the MEMS community.

Keywords: Additive manufacturing; MEMS; 3D printing; Microfabrication; Rapid prototyping.

1. Introduction

Microelectromechanical systems (MEMS) have been one of the well-established technologies over the past five decades, leading to the development of important devices such as piezo-electrics, accelerometers, inertial measurement units, sensors, micro-mirrors, micro gyroscopes microfluidics, micro-scale energy harvesting. MEMS are widely used in embedded systems and can be found in various applications such as automotive, aerospace, and communications. The key concept of MEMS manufacturing technology is the use of the top-down approach, which was initially developed for microelectronics, to fabricate microelectromechanical components and convert signals to chemical, mechanical, or biological responses. The global microelectromechanical systems market had grown from about $12 billion in 2014 to about $22 billion in 2020, and it is estimated to grow over the next few decades [1].

Additive manufacturing (AM) is part of the industry 4.0 technologies that have been advancing over the past 30 years. In 1986, Charles Hull introduced AM technology to create 3D objects by building them layer-by-layer through a stereolithography (SLA) process using a UV sensitive resin cured by UV light [2]. Following this, various AM technologies have been introduced, which have enabled the manufacturing of many of materials. The increasing demand for additive manufacturing technologies has triggered more investments to adapt these technologies into many industries [3]. In recent years, metals [4], polymers [5], and ceramics [6] in powder, filament, or liquid forms have been processed using additive manufacturing to fabricate products that have been adapted in many sectors such as defence [7], biomedical [8], energy [9], and aerospace [10, 11]. The growing demand for additive manufacturing research has been realised in the increased publications over the past 20 years, as depicted in Figure 1. The plotted data is obtained by searching the MEMS and additive manufacturing keywords in the past 20 years. The MEMS industry has found a fruitful opportunity to explore the potential of AM at various research levels. Teh et al. [12] and Vaezi et al. [13] introduced limited literature review papers of additive manufacturing technologies used for MEMS applications. However, as AM technologies have been innovating rapidly and become more mature in wide range of applications, especially in the past few years, this paper gives a timely and in-depth analysis of both MEMS conventional and additive manufacturing technologies of MEMS. The paper starts with reviewing the

conventional MEMS technologies, their applications, advantages and limitations. The second section of the paper is dedicated to the additive manufacturing technologies used in MEMS industries. Applications of using AM technologies in several MEMS applications are investigated in the third section. The potential and challenges of AM technologies are explained in the final section.

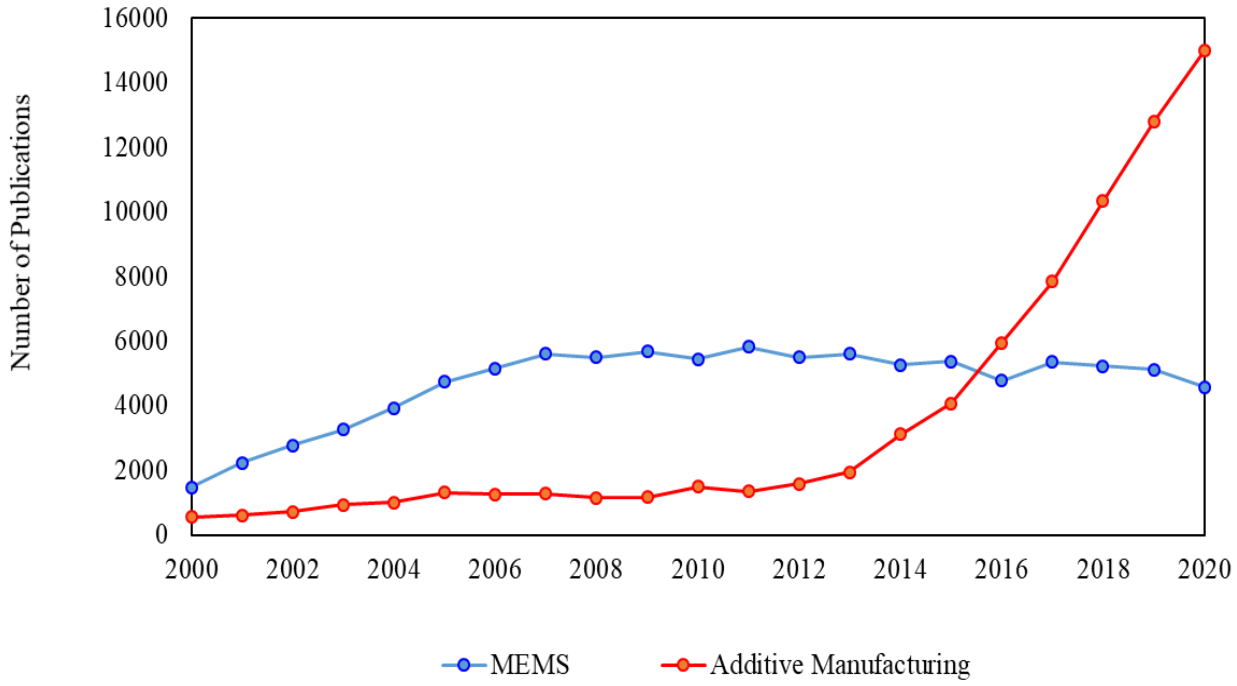

Figure 1: Research publications on MEMS and additive manufacturing from 2000 to 2020 (Source: Scopus.com).

2. Conventional Microfabrication Processes

Conventional microfabrication technologies comprise patterning, subtractive and properties modifications. Patterning techniques include UV photolithography, soft lithography, and microinjection moulding. UV lithography is one of the patterning techniques that uses UV to crosslink a layer of photosensitive resin through a patterned mask, selectively curing the required shape, and the uncured areas are dissolved (Figure 2a). Typically, silicon wafers are coated with a photosensitive resin layer with a thickness ranging from few microns to less than 2 mm using spinning or direct casting in a single or multiple layers. SU-8, one of the most popular photosensitive resins, has been used for many MEMS applications as it has favourable mechanical, optical, electrical, and magnetic properties which are based on the

processing conditions [14]. Unconventional photolithography techniques can be employed to create geometries more complex than typical 2D extruded shapes. For example, sealing caps packages can be obtained by using multiple photomasks with different patterning by exposing the top layer with UV, while the part underneath the cap was not exposed [15].

Soft lithography is a non-UV-lithographic technique in which a master mould containing patterned microcavities is used to produce microparts via replica moulding (Figure 2b). Soft lithography is a popular process as it is an inexpensive and simple approach to produce micropatterns with high accuracy. Soft moulds are usually prepared by pouring a curable prepolymer onto a solid mould, which can be prepared by using a UV lithography technique [16-23]. Several materials are used to prepare soft moulds, such as polyimides, polydimethylsiloxane, novolak, and polyurethanes [24-27]. Electrodeposition, on the other hand, refers to the deposition of suspended ions on a conductive electrode onto a micromould (Figure 2c). Suspended particles such as ceramics, metals, or polymers can be dispersed in the electrolyte suspension to improve the performance or the properties of the fabricated micro parts [28-32]. LIGA is one of the most popular microfabrication technologies. It refers to a German acronym that stands for (lithographie, galvanoformung, abformung), which means "lithography, electroplating and moulding". The UV-ray LIGA and X-ray LIGA are two common LIGA manufacturing processes. The two techniques are very similar; however, the X-ray LIGA technique uses X-rays to pattern high aspect ratio microparts in X-ray sensitive resins. X-ray LIGA is less popular as it requires the use of expensive X-ray synchrotron devices.

On the other hand, UV LIGA is a combination of both UV-lithography and electrodeposition. It starts with creating a micro mould on a conductive substrate using UV-lithography followed by electrodeposition of metal layers such as copper, nickel, or gold. Afterwards, the master mould is chemically or mechanically removed to achieve free-standing metal microparts. Microinjection moulding (µIM) technique is based on the well-known injection moulding approach. It is a mass production tool to manufacture 3D microparts from wide range of materials such as polymers, ceramics or metals. The manufacturing is conducted by injecting low melting temperature polymers into a mould containing microcavities, as presented in Figure 2d. Subsequently, the mould is cooled down, and then the micro components are ejected. Microcavities should be carefully designed to facilitate the ejection

process, especially with high aspect ratio microcomponents. The working temperature of this technique are typically less than 100 °C, and the injection pressure is in the range of a few bars. Metal and ceramics are typically used in injection moulding by loading the polymer feedstock with metal or ceramic powders by adding metal or ceramic powders. After injection, cooling down, ejection of the micro parts, debinding, and sintering steps are carried out to realise the consolidated metal or ceramic microparts [33-36].

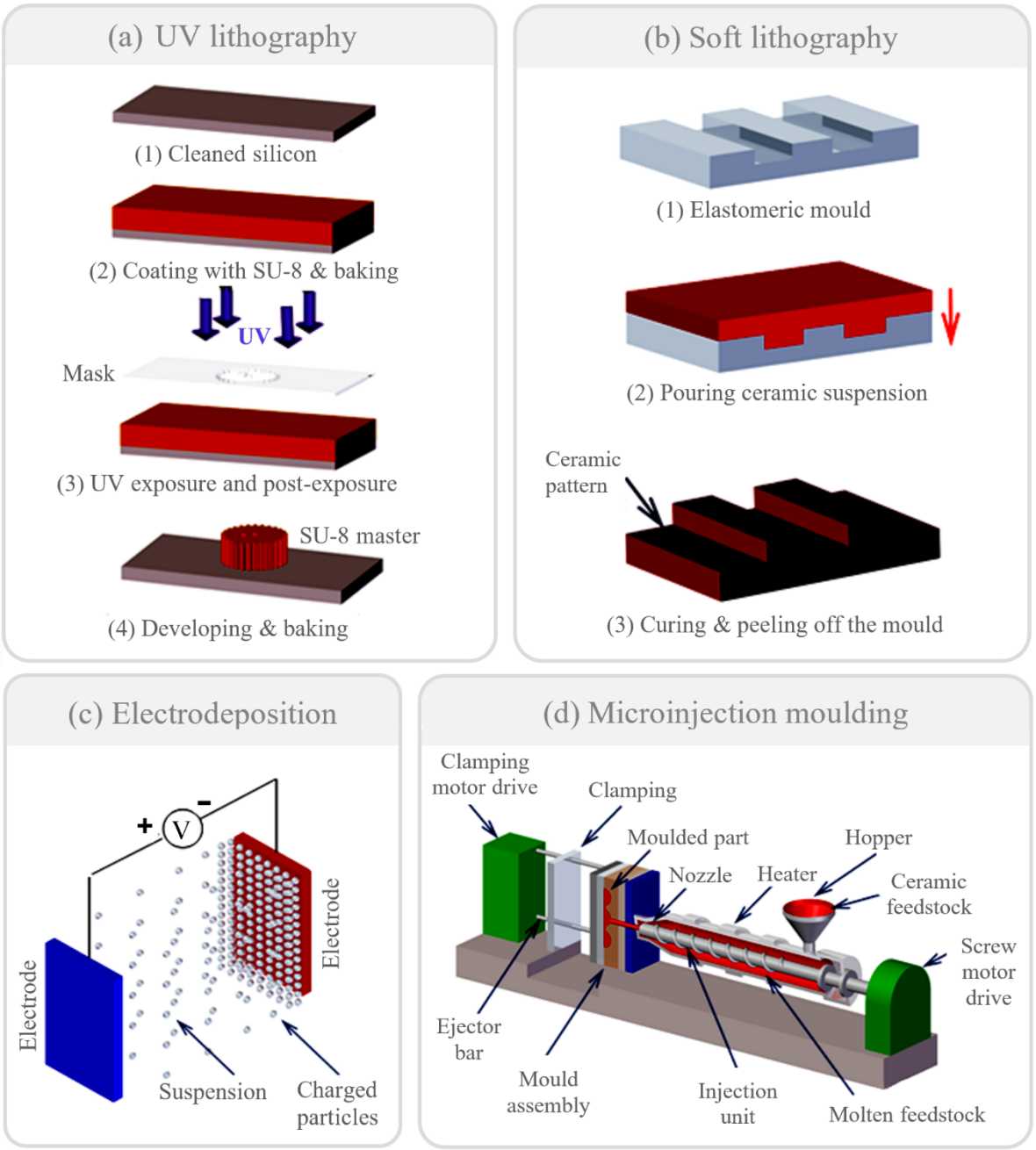

Figure 2: Patterning techniques including (a) UV Lithography, (b) soft lithography, (c) electrodeposition, and (d) microinjection moulding.

Subtractive methods include micro-electrical discharge machining (micro-EDM), reactive ion etching, and laser micromachining. micro-EDM is a technique at which an electrical discharge is created between an electrode and a workpiece. The electrical discharge is employed to erode the workpiece (Figure 3a) thermally according to a specific path. There are three micro-electrical discharge machining processes: hole boring, microwire EDM, and shaped working electrode [37]. In microwire EDM, a wire is drawn continuously to erode the workpiece [38, 39]. Hole boring is an EDM process at which the electrode is consumed, and hence it is compensated until the feature is patterned [37, 40]. One of the EDM disadvantages is the heat generated during erosion, creating a heat-affected zone [41].

Etching is another subtractive process that is used to remove the material through either wet or dry processes selectively. In wet etching, a liquid is used to dissolve unmasked areas of a wafer according to a specific micropattern [42]. On the other hand, dry etching refers to the use of reactive gases such as oxygen, boron trichloride, fluorocarbons, or chlorine to etch areas of the part. Focused ion beam is one of the dry etching processes that remove the material anisotropically or directionally by bombarding the substrate with ions [43, 44]. The technique can fabricate high aspect ratio microfeatures on the top of a wafer and free-standing microcomponents [70] (Figure 3b). Laser micromachining (LMM), also called laser ablation, is a laser beam subtractive method (Figure 3c). An advantage of laser micromachining is that it can pattern plastics, metals, ceramics, and glasses [45, 46]. The patterning takes place as the laser beam develops energy higher than the ablation energy of the workpiece. Various lasers can be employed using laser micromachinings such as excimer lasers and CO_2 and Nd: YAG lasers. Laser absorption depends on the reflection coefficient of the material, the angle between the workpiece surface and the laser, and the wavelength of the laser. MEMS systems fabricated using laser micromachinings include integrated sensors, circuits, detectors, and transducers [47-49].

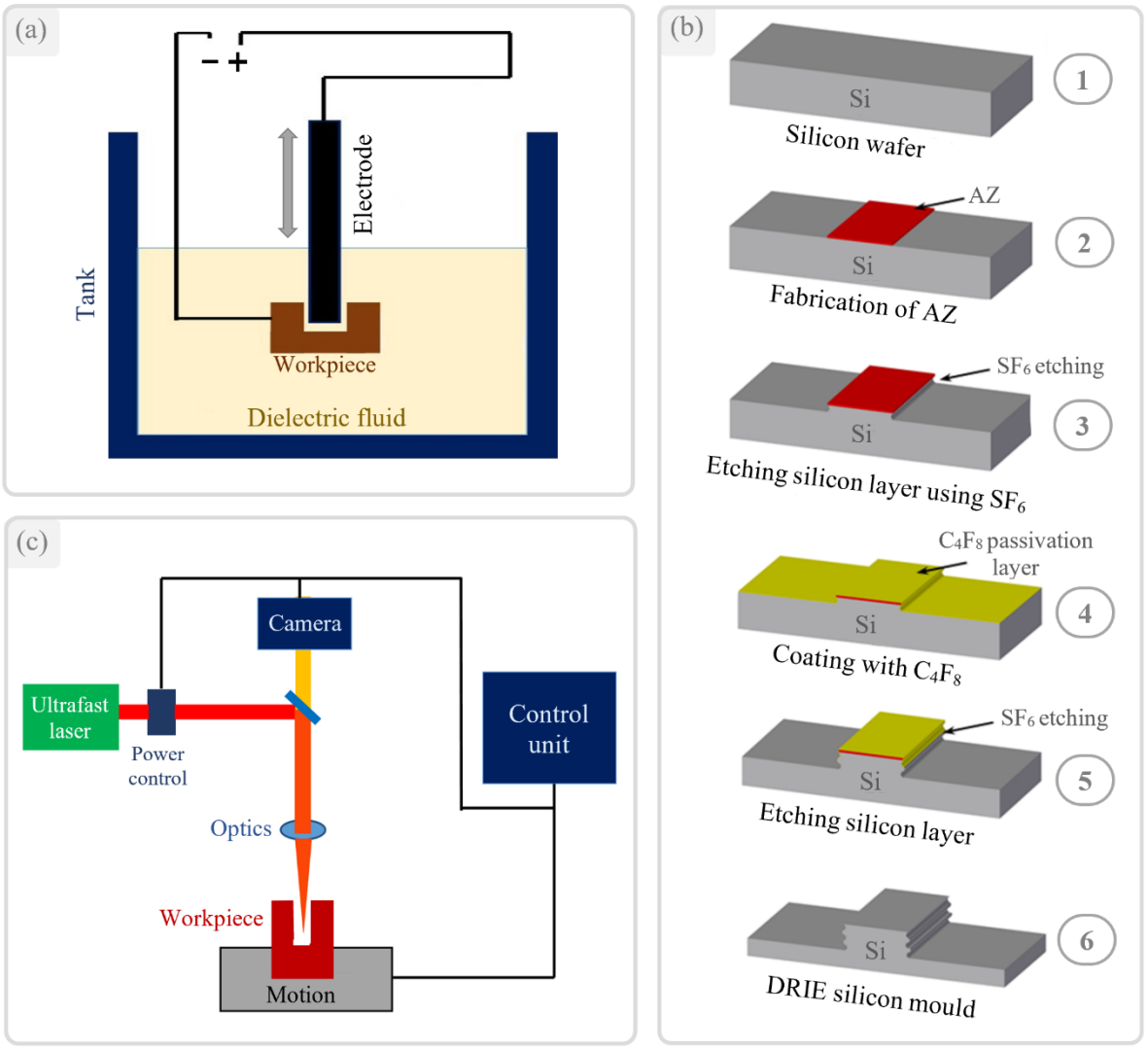

Figure 3: Subtractive techniques including (a) micro-electrical discharge machining, (b) deep reactive ion etching process, and (c) laser micromachining.

Properties modification techniques are physical vapour deposition, thermal oxidation, and chemical vapour deposition, see Figure 4. Physical vapour deposition (PVD) is used to deposit a thin layer of coatings such as thin metal films for MEMS applications. In physical vapour deposition, the material is evaporated and sputtered on a substrate's top surface. PVD is used in many applications such as semiconductors, solar panels, aluminised polyethylene terephthalate (PET) film, and titanium nitride for cutting tools. It is also used in decorations of trophies, toys, pencils, interior trims in automobiles, pens, and watchcases. Furthermore, PVD is used for antireflection coatings of optical lenses using magnesium

fluoride (MgF_2). The process takes place in reactors to deposit various metals, alloys, ceramics, and other inorganic materials (Figure 4a).

In thermal oxidation, an oxide layer is created on a substrate from a material such as silicon using water vapour or heated oxygen at a temperature of 700-1250°C. Firstly, an oxidised agent is diffused and reacted with the silicon wafer's top layer (Figure 4b). Wet-oxygen is capable of creating a thicker layer [50, 51]. The oxidising atmosphere may also include a small amount of hydrochloric acid that can eliminate metal ions present in the oxide layer. The reaction of thermal oxidation can be one of the following:

$Si + 2H_2O \rightarrow SiO_2 + 2H_2$

$Si + O_2 \rightarrow SiO_2$

In chemical vapour deposition, a chemical reaction between elements in an inert environment at a temperature of 300°C occurs to deposit a solid thin layer (Figure 4b). The process is typically used to form a layer of materials as silicon, carbon, titanium nitride, fluorocarbons, and tungsten. For silicon dioxide, it is worth noting that thermal oxidation is more efficient in creating a better quality layer when compared to CVD. The CVD of SiO_2 is realised by the reaction between silane (SiH_4) and silicon [1, 52, 53]:

$SiH_4 + O_2 \rightarrow SiO2 + 2H_2$

Chemical Vapour Deposition (CVD) can be categorised into plasma-enhanced chemical vapour deposition, low-pressure chemical vapour deposition, atmospheric pressure chemical vapour deposition, high-density plasma chemical vapour deposition, electron cyclotron resonance chemical vapour deposition, and atomic layer deposition. The process is widely implemented in the MEMS industry. For example, miniaturised transistors have been fabricated with a thin silicon dioxide layer deposited using CVD. Furthermore, the CVD of copper and low dielectric insulators of ($\varepsilon < 3$) have been recently carried out. Ceramics can also be deposited at a lower temperature than conventional powder processing and sintering. On the other hand, CVD has several disadvantages, such as the use of corrosive chemicals, pumping, and disposal equipment; moreover, the process involved the use of toxic, corrosive, flammable, and explosive gases.

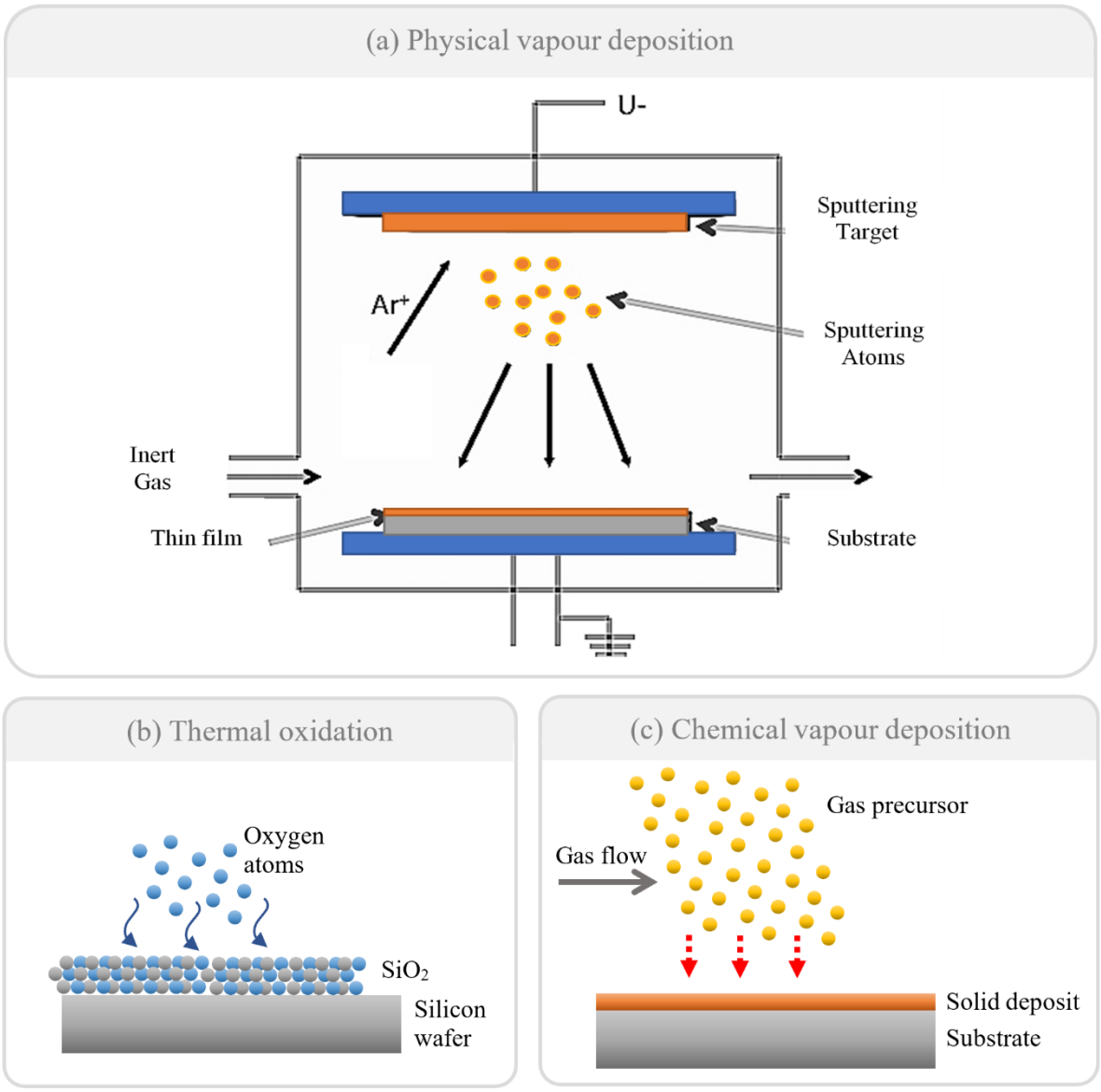

Figure 4: Schematic diagrams of (a) physical vapour deposition, (b) thermal oxidation, (c) and chemical vapour deposition.

This section showed that although MEMS microfabrication processes are diverse and capable of processing many different materials, the working principle of each of them restricts the geometrical complexity of the fabricated MEMS. In fact, these processes limit the MEMS fabrication to 2D (planer) manufacturing; in the best-case scenario, they can fabricate 2.5D structures. These techniques include patterning, subtractive and properties modifications technologies, which were initiated during integrated circuits (IC) development (listed in Table 1). In addition, most of the technologies mentioned above take place in dedicated micro/nanofabrication cleanrooms, which can only be found in well-funded

universities, research institutions, and niche industries. Therefore, the following sections will illustrate additive manufacturing potentials in microfabrication by reviewing their working principles, materials, and MEMs applications.

Table 1: Summary of conventional microfabrication processes

Technique			Resolution	Key limitations	Refs.
Patterning	UV Lithography		50 nm	▪ High capital and operating cost ▪ Limited materials used such as photoresists	[54]
	Softlithography (SL)		2 nm	▪ Limited set of materials used elastomers.	[55]
	Electrodeposition		100 nm	▪ Expensive for X-ray LIGA (both in capital and operating cost). ▪ Results depend on the deposition conditions.	[56]
	lithography electrodeposition and moulding (LIGA)	UV-ray LIGA			
		X-ray LIGA			
	Microinjection moulding (µIM)		100 nm	▪ Expensive capital and tooling cost. ▪ Carefully designed to facilitate the ejection process. ▪ difficult to design the cooling and ejection systems	[57]
Subtractive	Microelectrical discharge machining (µEDM)	Hole boring	200 nm	▪ The process limitation is the developed heat affected zone. ▪ Electrode wear ▪ Slow material removal rate.	[58]
		Microwire EDM			
		shaped working electrode			
	Deep reactive ion etching	Wet etching	150 nm	▪ Expensive capital cost. ▪ Low Etch Rate ▪ Low level of selectivity ▪ Surface damage	[59]
		Dry etching			
	Laser micromachining (LMM)		50 nm	▪ Expensive capital cost. ▪ Laser absorption depends on laser wavelength and reflection coefficient. ▪ The angle between the workpiece and the laser affects the absorbed energy.	[60]
Properties modification	Physical vapour deposition (PVD)		10 nm	▪ Expensive capital cost and a reactor is needed ▪ Line of sight' limitation ▪ Requires a cooling water system	[61]
	Thermal oxidation		100 nm	▪ A high temperature is required; ▪ Limited set of high-temperature materials.	[62]
	Chemical vapour deposition(CVD)		10 nm	▪ Corrosive chemicals usage along with the controlled process, special pumping, and disposal equipment ▪ Gasses are toxic, corrosive, flammable, and explosive ▪ Poor quality of the deposited layer	[63]

3. Additive Manufacturing of MEMS

Additive manufacturing - widely known as rapid prototyping or three-dimensional printing, is based on several approaches to create 3D objects incrementally according to a digital model. The digital model in an STL form is loaded into a 3D printer, oriented, and is sliced into specified layers. Next, the printer starts to build the object following the path of a specific G-code. Additive manufacturing has been developed to adapt the technology throughout research work and industrial applications [64-67]. This section explains the leading AM technologies used in MEMS and their main features.

3.1. Microsterolithography

Microstereolithography (μSLA) is a light-based technique that uses photosensitive polymers, which can be cured upon exposure to Ultraviolet (UV) rays. Microstereolithography has several benefits, such as high accuracy, low cost, and the capability of processing several materials. In microstereolithography, a localised photopolymerisation process takes place by incrementally exposing layers of a photosensitive polymer to UV. During the UV-polymerization, free radicals are activated and then crosslink strands of monomers to form solid hydrogels. Microstereolithography is available in three forms. The first technique is the single-photon polymerisation microstereolithography, which provides sub-micron resolution with a small throughput as the UV scans the resin layer point-by-point. In single-photon microstereolithography, a UV laser scans photosensitive resin in a tank and starts the photopolymerization process. A computer numeric control and a computer-driven shutter are used to control the laser, ensuring that the photopolymerisation process is conducted correctly, as shown in Figures 5a and b. During printing, the building platform moves slightly under the resin surface to create a thin layer. Next, the UV beam scans the layer and initiate the photopolymerisation process. Afterwards, the platform moves down and creates a second layer on top of the first one. The UV repeatedly scans the newly formed layers according to the digital model. Suppliers of SLA technologies such as Formlabs and Elegoo use a bottom-up building system, where the building substrate is immersed in a resin tank, creating a thin layer on the bottom of the tank. A UV beam scans upward from below through a window at the tank's bottom. After the completion of the building process, the print is removed and soaked in a solvent to dissolve the uncured resin. One disadvantage

of the single-photon approach is that it is time-consuming as the UV scans the resin layer point-by-point.

The resolution in the horizontal plane is limited to the UV beam size, which is in the range of ten micrometres.

Two-photon polymerisation microstereolithography was introduced to manufacture higher resolution parts at a nano-scale level. In this technique, a resin molecule absorbs two photons using an ultrafast laser, as shown in Figures 5c and d. Similarly, this leads to resin molecule curing of the through a photopolymerisation process. The process is one of the most high-resolution fabrication processes that have been used to fabricate complex microstructures for MEMS and advanced photonics. One of the advantages of using two-photon microstereolithography is that it can print inside the resin rather than being limited only to the surface. Typically, the resin is sensitive to UV, but it has low absorbance in the visible light and near-infrared range. Therefore, using single-photon microstereolithography can only crosslink the surface of the photosensitive polymer, whereas the near-IR light in the two-photon microstereolithography can penetrate further into the photosensitive polymer and crosslink deep inside the resin.

The projection microstereolithography approach provides a dynamic stereolithography mask through digital light processing (DLP) that act as a virtual mask. The process uses UV to crosslink the whole layer with a micro/nano-scale resolution. The DLP unit has the ability to control the light intensity of each pixel, which allows good control over the crosslinking process and hence the printed microstructure properties. Several forms are available based on projection microstereolithography, such as liquid-air interface polymerisation and liquid-substrate polymerisation. There are two major challenges of projection microstereolithography techniques. The first one is the slow printing rate, whereas the second one is the presence of the stair-stepping surface between layers (Figure 5e and f). Continuous liquid interface production (CLIP) was recently introduced to produce mesoscale parts with microfeatures of (≈50μm) at high speeds of up to 7 mm/min. The technology is based on employing an oxygen-permeable Teflon window to prevent resin crosslinking in the oxygen-rich dead zone and enables crosslinking only above that zone. This allows the

continuous feeding of resin at the building surface, which is below the dead zone. Therefore, rapid printing and stair-stepping free structures can be created.

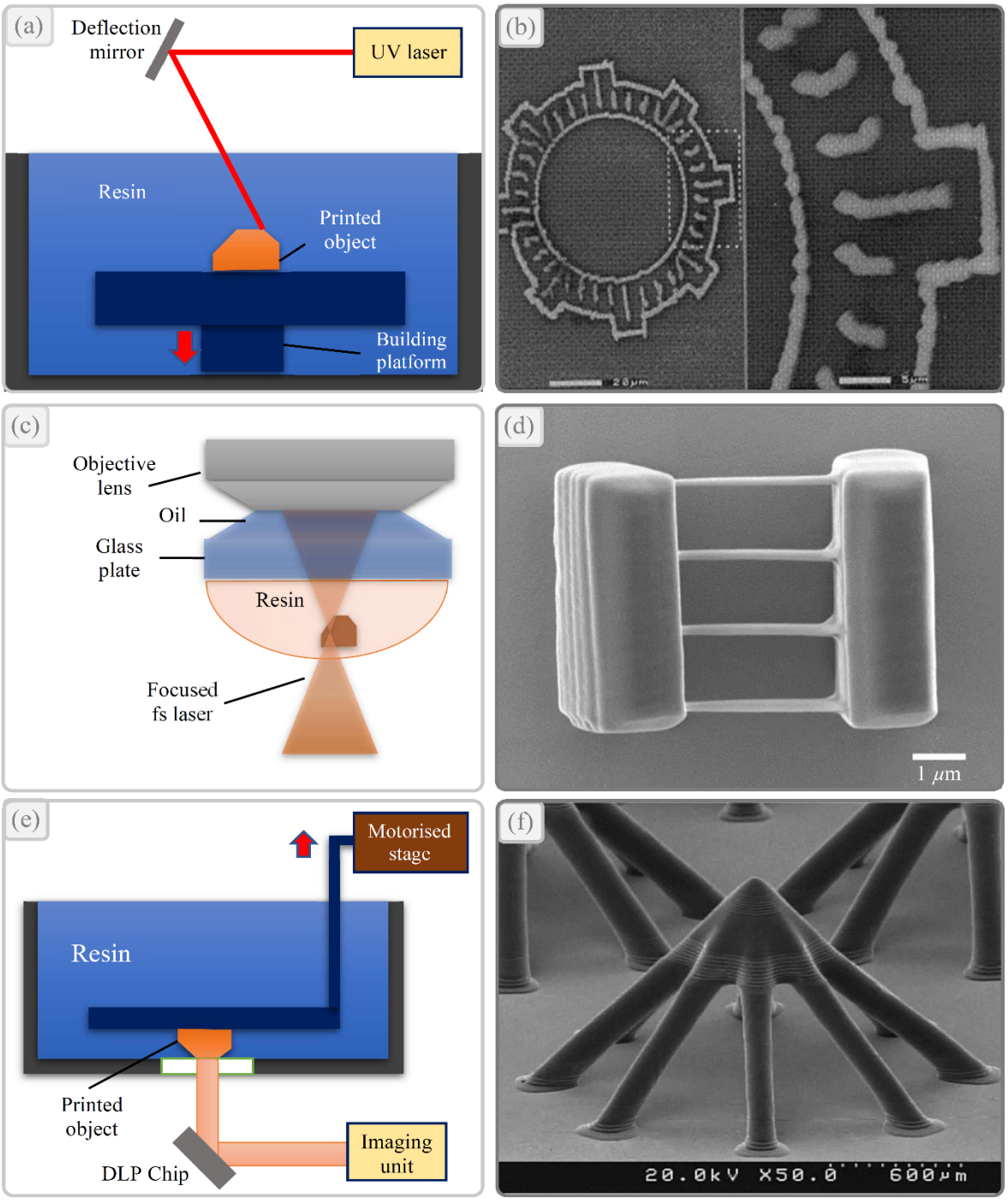

Figure 5: (a) Single-photon µSL. (b) A 400 µm microgear with 2 µm line width fabricated by standard single-photon µSL process, Reproduced with permission [68] 2021, Elsevier . (c) Two-photon µSL. (d) A TPP-printed four-bridge structure fabricated by the TPP process, Reproduced with permission [69] 2021, springer nature. (e) The projection µSL. (f) A multi-thickness object created using the projection µSL, Reproduced with permission [70] 2021, springer nature.

3.2. Laser Microsintering

Laser microsintering is a powder bed fusion approach in which a focused beam of laser is applied to sinter a thin powder layer and create a 3D component in the layer by layer according to a digital CAD design. Laser microsintering is a modified selective-laser-sintering (SLS) technology. The first attempts were made using submicron powder at which was scanned using a continuous laser beam with a focus diameter of 14 microns. These experiments were unsuccessful as there was no bonding between the printed layers and the building substrate [71]. In addition, the molten material formed discrete droplets distributed sparsely. These issues were due to the microparticles' loose packing density and the low vapour pressure inside the building chamber. The use of q-switched laser pulses alleviates these challenges as it yields higher laser intensity compared to continuous laser. Microparts with a 50 µm feature size, an aspect ratio of about 10, and a surface roughness (*Ra*) of 1.5µm were successfully achieved using this modified laser setup. In addition, the improved process is implemented with a raking process to create a very thin layer of powder. Several materials can be processed using laser microsintering, including metals (e.g. Al, Ti, Cu, and Ag), ceramics (e.g. lead zirconate titanate, silicon carbide, and alumina) and polymers [71]. Figure 6a shows a schematic of laser microsintering. Typically, laser microsintering produces microparts with a relatively coarse texture and poor surface quality. This is because of the presence of local irregularities of the powder particles, the limited powder packing, the low wetting properties of smaller powder particles, and the low sintering density. Besides, the high surface area of the small-sized particles promotes the reaction with oxygen and humidity in the building chamber. It is necessary to use sealed and oxygen-free building chambers, finer particles, optimisation of process parameters, and special powder handling systems. Roy *et al*. developed an improved laser microsintering process and was able to fabricate 3D metal microparts with a building rate of 60 mm^3/hour and resolution of 5 µm [72]. Examples of using this process are presented in Figures 6b and 6c. The technique is ideal for the fabrication of free-standing ceramic and metal microparts.

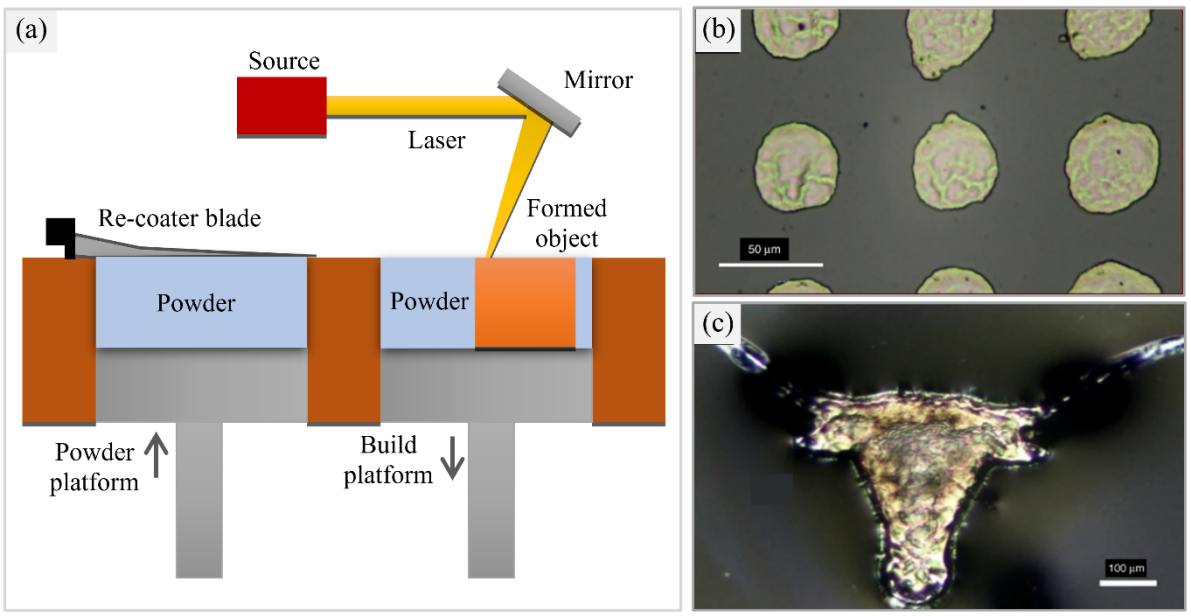

Figure 6: (a) Laser microsintering process. (b) Optical microimage of a 40 µm diameter array. (c) Optical microimage of the logo of the University of Texas with a minimum feature of 7 µm, Reproduced with permission [72] 2021, springer nature.

3.3. Laser-Induced Forward Transfer

The laser-induced forward transfer is an additive and non-contact technique that can fabricate high-resolution micropatterns of functional and structural materials through the deposition of micro amount of a material into a substrate without the need for masks or nozzles. The technique has a limited capability to print complex 3D structures. The technique works the same way as the drop-on-demand process, which allows the printing of several solids as well as low-viscosity fluids [73]. In this technique, a laser beam is employed to hit ink coated transparent Mylar tape and transfer the inks onto a substrate (Figure 7a). The process was further developed by Bohandy *et al*. by employing a pulsed laser to deposit copper microlines on silicon oxide. The authors studied the effect of laser energy on the thickness of the deposited copper using the Nd:YAG laser. The setup developed by Bohandy et al. is very similar to the current Laser-induced forward transfer systems [74]. The technique was initially considered to be promising in MEMS. However, the complex design and the system cost until recently have not supported this technology's penetration into several industries. This is in addition, the inability of this technique to produce true 3D shape. Several materials are processed using laser-induced forward transfer,

such as polymer, ceramics, metals, composites, or cell culture. Typically, femtoseconds ultrashort-pulsed laser is used to reduce the developed heat-affected zone, which causes undesirable oxidation and phase changes [75]. The process enabled high aspect ratio parts manufacturing with a resolution of 0.5 μm and a printing rate of about 1000 mm/s. Figure 7b shows an example of a microgripper fabricated using laser-induced forward transfer [76].

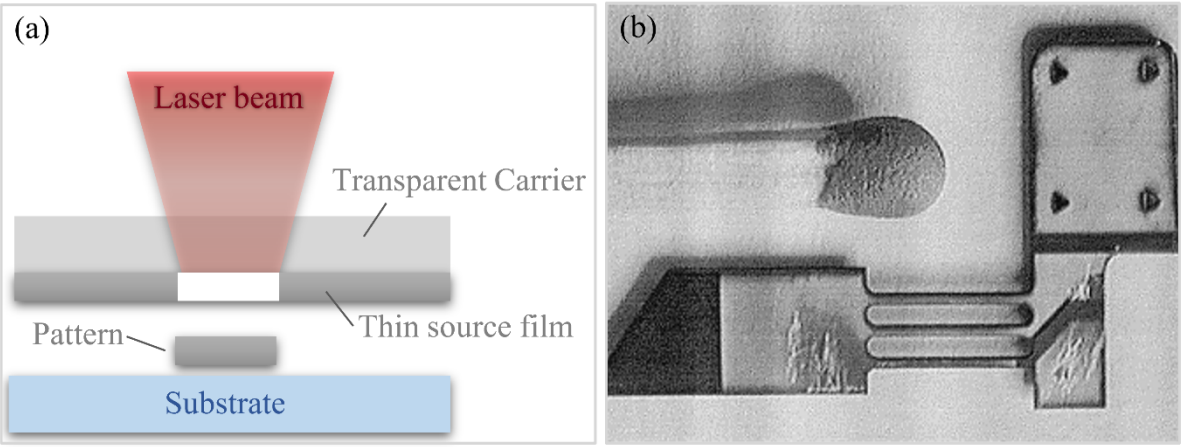

Figure 7: (a) Laser-induced forward transfer process. (b) Optical microimage of an electrostatic microgripper, Reproduced with permission [76] 2021, Elsevier.

3.4. Material Extrusion

Material extrusion (ME) is one of the most common additive manufacturing technologies due to its availability in desktop versions to hobbyists, simplicity, and low cost. In ME, the material is deposited from a nozzle and build up parts incrementally according to a designed model. Figure 8a presents a schematic of the ME approach. Different materials, such as thermoplastic polymers can be processed using this technique, as in fused deposition modelling. Whereas gels and pastes are processed pneumatically or by using a syringe. In fused deposition modelling, the material must be softened first through heaters before being extruded [77]. The quality of the FDM-printed objects is typically affected by the material properties, nozzle diameter, deposition speed, geometry, layer thickness, nozzle temperature, and the building substrate temperature. However, it is difficult to print components with a layer thickness smaller than 16 μm due to polymer melts' viscoelastic behaviour. Material extrusion is also capable of depositing multi-materials by using two or more

nozzles fed with different materials filaments. Robocasting (RC) is a syringe based type at which a ceramic suspension is extruded to shape ceramic MEMS. It is a reliable 3D printing technique of MEMS to fabricate dense ceramic MEMS with complex and fine details, Figure 8b [78].

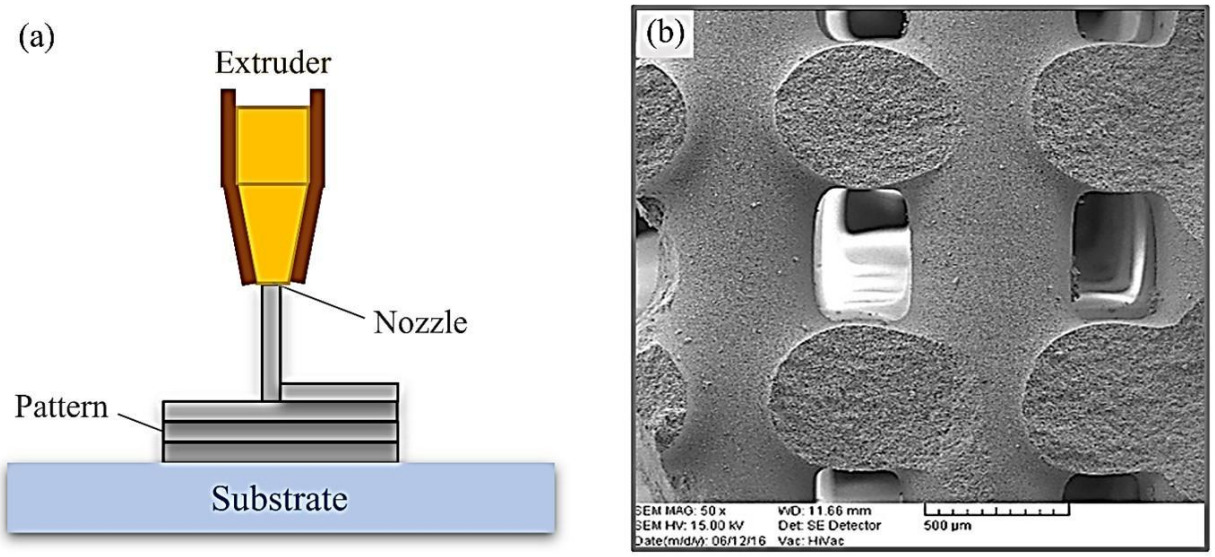

Figure 8: (a) Materials extrusion process. (b) SEM images of a ceramic scaffold fabricated using robocasting, Reproduced with permission [79] 2021, Elsevier.

3.5. Material Jetting

Material Jetting is based on the conventional inkjet process whereby printheads are used to deposit a liquid photosensitive polymer on the building platform layer by layer. Continuous or Drop-on-Demand (DOD) inkjet approaches are two forms of material jetting techniques. However, drop-on-demand is more used for 3D microfabrication, as there is more control over the deposited material. Currently, several desktop inkjet printers are available such as Fuji Dimatix 3D printer, which is able to 3D print parts at micrometre levels. Figure 9a presents a schematic diagram of material jetting and an example of using inkjet printing in microfabrication. Material jetting method has been one of the most widely used processes because of its productivity and reliability. The first drop-on-demand inkjet printing was introduced in 1970s. Following this, many forms of drop-on-demand inkjet 3D printers became available. In this technique, ink drops are deposited by the impact of the pressure wave induced by piezoelectric actuators [80]. Push mode, squeeze mode, shear

mode, and bend mode are different deformation modes triggered by piezoelectric actuators to control the ejection of the ink [81]. Multijet printing is another form of materials jetting at which more than one material is ejected. The technology is capable of 3D printing parts in full colours and good surface quality. It is also can print polymer materials by jetting the material droplets through a printing head. Wax can be used to support over hanged features, which offers an excellent surface quality of the printed parts. Polymer materials such as polymethyl methacrylate, polycarbonate, polypropylene, polystyrene, and high-density polyethene are widely used in this technique. Besides, ceramic slurries composed of ceramic powders, dispersants and binders are also to shape dense green parts followed by a sintering process [82]. However, there are several restrictions of ink materials, such as rheological and solidification characteristics in order to be able to achieve desired print specifications. This can be achieved by having inks with an adequate shear thinning and a constant cross-section of the ink being desisted so that they can achieve an acceptable structural rigidity after 3D printing [83].

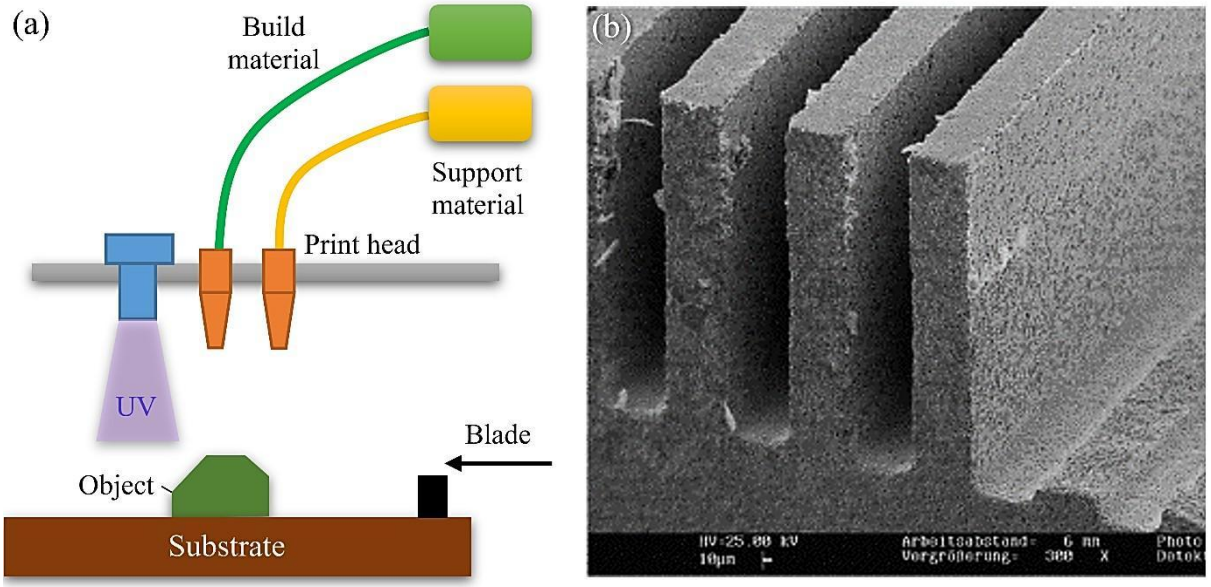

Figure 9: (a) Materials jetting process. (b) SEM images of a ferroelectric PZT ceramic with micromachined actuating elements, Reproduced with permission [81] 2021, Elsevier.

3.6. Sheet Lamination

In sheet lamination, the sheets of material are cut using a laser beam or a mechanical cutter, stacked, and bonded together using heat energy or glue. When

the bonding is carried out using ultrasonication, the process is also called ultrasonic additive manufacturing, whereas it is called laminated object manufacturing if the glue is used in the bonding. Figure 10a presents a schematic diagram of the sheet lamination process. Sheet lamination has several advantages, such as processing a diversity of materials, composites, and graded materials. In addition, sheet lamination is productive, inexpensive, and robust. However, there are several drawbacks with this technology especially when it is used for microfabrication purposes. This includes the poor resolution of the printed objects, the use of thin sheets of material, and the need for a suitable binder. Sheet lamination was employed to manufacture microreactors, microsensors, heat exchangers, and micro-fuel cells. Luong et al. [84] used sheet lamination supported with laser-induced graphene to explore the fabrication of 3D graphene objects. Laser-milling was also used to enhance the quality of the printed components. The produced graphene foam objects show good mechanical strength and electrical conductivity, which indicates great potential in the development of flexible electronic sensors and energy storage systems [84]. Figure 10b shows a laser-induced cube made using sheet lamination and fibre laser milling.

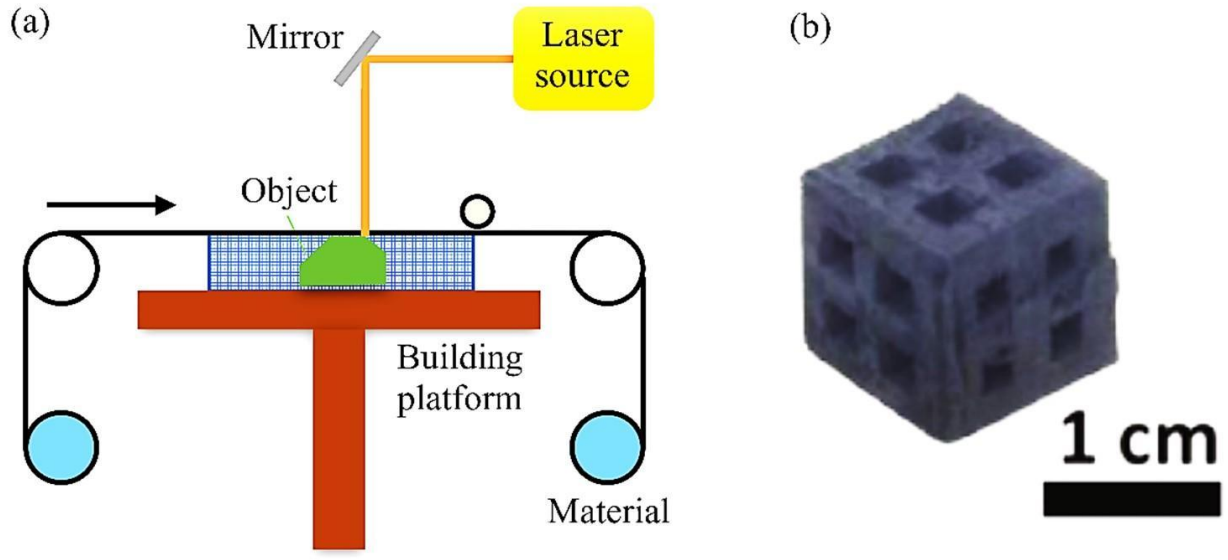

Figure 10: (a) Sheet lamination process, (b) 3D Laser-induced graphene foam 3D printed by using sheet lamination and fibre laser milling, Reproduced with permission [84] 2021, John Wiley & Sons, Inc.

Table 2 contains a summary of the additive techniques used in MEMS and their main features that have been investigated in this section.

Table 2: Summary of additive manufacturing used for microfabrication

Technique	Resolution	Layer Thickness	Materials	Micro Parts	Refs.
Projection Micro stereolithography (PμSL)	100 nm	4 μm	UV-curable resins, UV-curable resin mixed with ceramic nanoparticles	■ Periodic arrays ■ Microlattices ■ Microrotors ■ Microgears ■ Microturbines	[70, 85-92]
Two-photon polymerization (TPP)	23 nm	100 nm	UV-curable resins, UV-curable resin of polymer-ceramic hybrid material	■ Microlenses ■ Microturbine ■ Microrotors	[93-95]
Continuous liquid interface production (CLIP)	50 μm	No layers	UV-curable resins, UV-curable resin mixed with ceramic nanoparticles, ceramics polymers	■ Micro-rods ■ Micro-lattices	[96-98]
Fused deposition modelling (FDM)	100 μm	32 μm	Polymers, ceramics, metals	■ Microfluidic devices	[99]
Pneumatic Materials Extrusion	76 μm	100 μm	Al_2O_3, SiO_2, Mullite, Bioglass, Y_2O_3/ZrO_2, Si_3N_4, SiC,SiO_2/glass, HA, TCP, B4C, $BaTiO_3$, ZnO,	■ Micro-lattices ■ Micro-channels ■ Scaffolds	[79, 100]
Ink-jet printing	<1 μm	1 μm nozzle diameter	UV curable resins, silver and ceramic filled ink	■ MEMS cantilevers ■ Scaffolds with micro sizes pores ■ RFantennas	[101-103]
Laser micro sintering (LMS)	5 μm	1.5 μm	Metal, ceramics, polymers	■ Micro springs ■ Catalyst beds with micro lattices ■ Free-standing walls ■ Microturbines	[6, 72, 104-107]
Laser-Induced Forward Transfer	0.5 nm	190 nm	Metal, ceramics, polymers, cells	■ Microbridges ■ Microgrippers ■ Microcantilevers	[73-76, 108-110]
Sheet lamination (SL)	-		Si-SiC	■ Microgears	[111]

4. Applications

4.1. Microelectronics and Circuitry

Additive manufacturing of microelectronic devices and circuitry offers an attractive manufacturing route by allowing flexible and large-area devices at a low cost which add more functionality to those miniaturised systems. The majority of the techniques used for microelectronic and circuitry is based on the adaptation of pneumatic material extrusion to develop microelectronics devices, whereas few research studies were found on the use of microstereolithography, laser microsintering, and inkjet printing. Electronic and electrical circuits can be integrated into embedded structures due to the layer-by-layer concept of additive manufacturing. Robinson *et al*. used pneumatic material extrusion and ultrasonic consolidation to 3D print a cellular aluminium board with an integrated panel. The printed circuit was fully embedded in the lightweight structure, eliminating the need for vias and cabling ducts. Besides, the encapsulation of the circuits protects the system from the environment [112].

Conventional manufacturing methods, as discussed in section 2, such as lithography, are typically made by using flat substrates made of silicon or glass. However, building or patterning electronics on conformal geometries greatly benefit from creating complicated nano/microdevices. Adams *et al*. [113] investigated the use of material extrusion technique to 3D print a silver antenna conformed to concave and convex substrates with a performance similar to the Chu limit (Figure 11a). Zhou *et al*. [114] extended this methodology to fabricate 2D and 3D printed passive radiofrequency devices such as transformers, inductors, and oscillators using silver ink (Figure 11b). The developed technique can produce compact microelectronic features on complex geometry substrates, which enhanced their mechanical integrity. Moreover, conformal additive manufacturing enabled fixable devices such as wearable antennas, sensors, and electronics. A laser-based pneumatic material extrusion system was employed by Skylar-Scott *et al*. [103] to fabricate improved 3D printed conductive components. The laser beam's role is to selectively anneal the deposited inks during the material extrusion, which enabled the fabrication of complex and free-standing geometries on both rigid and flexible substrates. Another extension of this approach was introduced by Liu *et al*. [115] to develop 3D printed porous $LiFePO_4$ electrodes. The printed materials were

deposited into a chamber kept at a low temperature and set to retain the mechanical integrity and the geometry of the 3D printed electrodes. Next, the solvent is removed by freeze-dried in order to achieve conductive electrodes with high porosity [115]. Additive manufacturing was also implemented to fabricate electronics, which enables discreet data collection. Medina *et al*. [100] introduced both microstereolithography and material extrusion to place a camera and video transmitter inside a printed alarm clock structure which shows the ability of AM to realise products with complex shape geometries and discreetly embedded electronics [116]. An integrative additive manufacturing approach was presented by Liu et al. [117] for rapid MEMS fabrication using different materials. With a multi-extruder 3D printer insulation, conductive and soluble materials can be simultaneously used to successfully 3D print capacitive force sensors with a relatively complex suspended beam-plate structure in a one-step process without the use of any metallization, alignment, and assembling techniques. The proposed integrative additive manufacturing process of the capacitive force sensor was completed in less than one hour and the fabricated senor has been used successfully blood pulse monitoring [117].

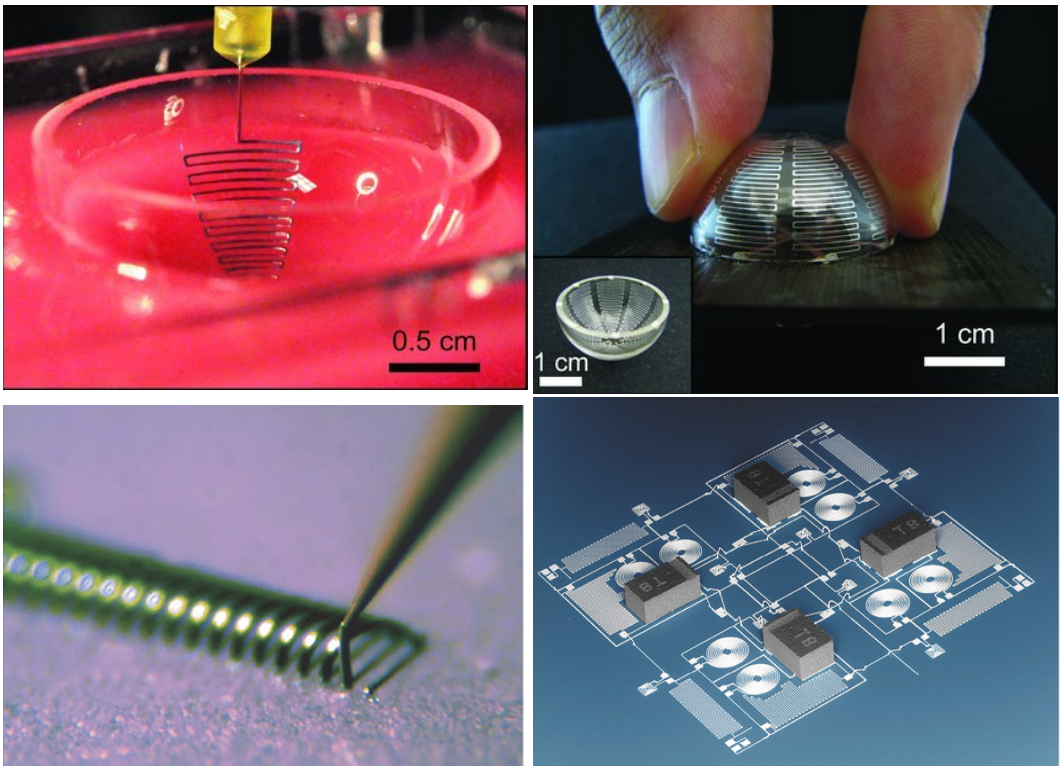

Figure 11: (a) An antenna being 3D printed onto a convex glass substrate embedded in a PDMS mould. (b) The antenna before inset and after connection, Reproduced with permission [113] 2021, John Wiley & Sons, Inc. (c) Direct writing of a silver ink using a 10 µm nozzle. (d) Assembled self-sustained oscillators, Reproduced with permission [114] 2021, John Wiley & Sons, Inc.

An integrative additive manufacturing approach was introduced by Liu et al. [117] for the rapid fabrication of MEMS devices using different materials. With a multi-extruder 3D printer insulation, conductive and soluble materials can be simultaneously used to successfully 3D print capacitive force sensors with a relatively complex suspended beam-plate structure in a one-step process without the use of any metallization, alignment, and assembling techniques. The proposed integrative additive manufacturing process of the capacitive force sensor was completed in less than one hour and the fabricated senor has been used successfully blood pulse monitoring, see Figure 12 [117].

Several researchers have investigated approaches such as microstereolithography, direct light processing, and laser microsintering to create conductive traces and structures. Microstereolithography was implemented to print conductive and elastic composite hydrogels [118]. On the other hand, direct light processing was used for the 3D printing of multiple materials, including carbon nanotubes with controlled conductive and non-conductive areas [119]. The two-photon polymerisation of a polymer-gold composite resin was used to achieve gold microstructures, whereas selective laser sintering was employed using a carbon nanotube polyurethane nanocomposite to achieve printed structures with a conductivity of about 10 Ωm using 1% of CNTs [120]. The feasibility inkjet 3D printing was carried out to manufacture miniaturised Li-ion of a thickness of fewer than 10 µm for miniaturised power batteries. The authors optimised the ink composition in terms of viscosity, contact angle, and surface tension to achieve a stable aqueous suspension suitable for injection printing [121]. Roy *et al*. developed an improved laser microsintering process capable of producing 3D metal circuitry suitable for microelectronic applications [72]. A laser-induced forward transfer technique was used to fabricate selective prenucleation using palladium on a quartz substrate. The thickness of the printed palladium was only a few nanometres [122].

The developed porosity in the printed conductive features is a typical issue that may cause electrical shorts within the same layer or between stacked layers. Process optimisation was used to optimise the process parameters and the conductive inks so that they can be directly printed with an improved resistivity of the silver inks [123]. Another solution, introduced by Wu *et al*. [124], is by the use of AM techniques to pattern micro-channels that can be filled with conductive ink. The challenge here was that the conductive inks require heating at a temperature above 100°C to remove the solvent, densify the ink, and enhance conductivity. However, a small number of polymers can work at temperatures more than 100°C, such as Duraform for selective laser sintering, Prototherm for stereolithography, and ULTEM for FDM. High temperatures allow sintering of the deposited particles to form necks and enhance densification, which promotes the conductivity of the printed circuits. A resistivity of 4.3×10^{-8} Ωm was achieved using local annealing, which is similar to the bulk silver resistivity. Another issue is the poor bonding between the deposited material and the substrate, which may cause delamination. As a result, it is challenging to repair delaminated circuits, especially in the case of embedded circuits. Systems from Stratasys and Optomec use a UV curable resin as an interlayer binder between the FDM surface and the conductive ink which interlayers are bonding the [125].

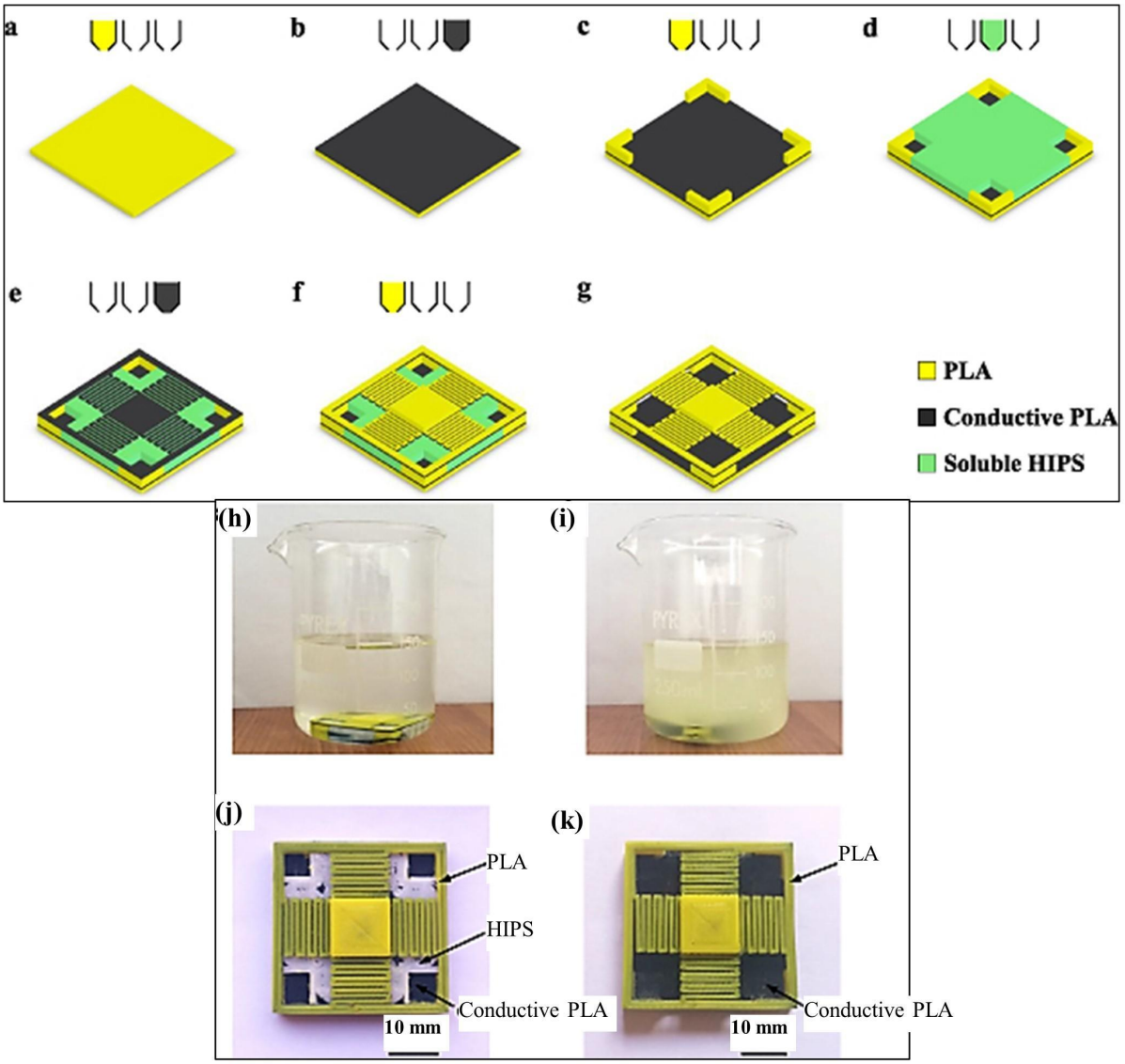

Figure 12: The integrative 3D printing of (a) bottom plate, (b) bottom electrode, (c) Spacer, (d) support, (e) top electrode, (f) top plate, (g) removal of support, Images of (h) The printed model in the D-Limonene solvent, (i) dissolve of HIPS support, (j) the device after 3D printing, (k) after removing the support, Reproduced with permission. [117],2021, IOP Publishing, Ltd, Inc.

4.2. Packaging

Most MEMS devices must be attached, integrated, and packaged with integrated circuits (ICs) as a part of a larger micro/macro electronic system. MEMS typically carried out a function such as sensing, actuating, etc., whereas ICs process the signals and preforms functionalities such as amplification, filtering, noise removals, etc. MEMS packaging is defined as the post-processing integration of MEMS after microfabrication. Once MEMS devices are released, processes such as encapsulation, dicing, wire bonding, and assembling

can be utilised for packaging. For example, MEMS devices may be packaged and sealed in silicon, glass, or ceramic packages to prevent the systems from exposure to oxygen, moisture, or dust. The additive manufacturing of plastic packaging on silicon wafers is one of the basic forms of 3D printed packaging. The typical layer thickness of 50-200 µm of many 3D printers falls within the range of the building containment of the commercially available glass and silicon wafers. The additively manufactured packaging may contain the MEMS devices fully or partially for a further sub-assembly step. Similar to the fabrication of microelectronics, adhesion to the substrate is an important consideration when selecting the additive manufacturing process. Adhesion layers may be introduced to enhance the bonding of polymers to the substrate.

The feasibility of MEMS packaging fabricated using additive manufacturing was demonstrated by several researchers. Goubault *et al*. [126] studied the use of stereolithography and fused deposition modelling to print the packaging onto the MEMS locally. The fused deposition modelling showed a very poor adhesion onto the silicon substrate, and no optimum conditions were found to improve it. The stereolithography technique was found to be promising in terms of adhesion and shape resolution. The same authors extended the study using the stereolithography process. The benefit of using a transparent resin in the SLA process was to allow controllable transparency of the printed packaging. The authors applied process optimisation and investigated the effect of relaxation time and post-processing cleaning on the shape and dimension of packaging. In addition, they found a low bonding strength of the 3D printed packaging [127]. A similar investigation was performed by Tehrani *et al*. [128] to investigate the utilisation of stereolithography in MEMS packaging. The polymeric and ceramic loaded resin was 3D printed. The E-band of 55-95 GHz was investigated with respect to the loss tangent and relative permittivity. It was found that the relative permittivity of the printed packaging was within the expected limits, whereas an improvement in the permittivity of the loaded ceramic resin was observed. Besides, no visible cracks or distortion due to thermal stresses were found in the samples. Packaging for die encapsulation and antenna arrays were demonstrated as a proof of concept. A CO_2 gas sensor filtering packaging was manufactured using a multijet 3D printer. The developed packaging has the ability to prevent dust particles using the anodic aluminium oxide membrane as a filter (Figure 13a and b). The use of an anodic aluminium

oxide filter caused a response delay, which was acceptable and proved to protect the system from dust particles. The inkjet printing approach used in this research can also be extended to a wide range of sensing applications [129]. Fan-out wafer-level is an integrated packaging technique that further enhances conventional wafer-level packaging solutions by reducing the packaging size and enhanced electrical and thermal conductivity compared to standard packages. A drop-on-demand inkjet printing for Fan-out wafer-level packaging is a promising approach to manufacture capacitive micromachined ultrasound transducers (CMUT). Typically, inkjet printing is limited to low viscosity inks. As a result, silver particle-loaded inks yield a thin layer as most of the ink content is evaporated, and the technique was shown to be powerful and cost-effective for MEMS packaging [83].

A powder bed fusion process with a powder layer thickness of 20-40 microns was used to fabricate Grade 316 stainless steel packaging for millimetre-sized batteries (Figure 13c and d). The packaging thickness was chosen to be 200 µm to maintain a good compression between the cathode and anode. Urethane resins were used to seal the integrated MEMS from moisture, chemical, biologic organisms, salts, and dust as well as providing a good level of mechanical strength. The developed packaged millimetre batteries showed appropriate compatibility for energy harvesting [130]. Although research on packaging using additive manufacturing has not been well established yet, the obtained results showed that the integration of additive technologies into packaging systems enables the development of fully printed-on-demand packaging for different MEMS products such as batteries, sensors, radars, and 5G mobile communications.

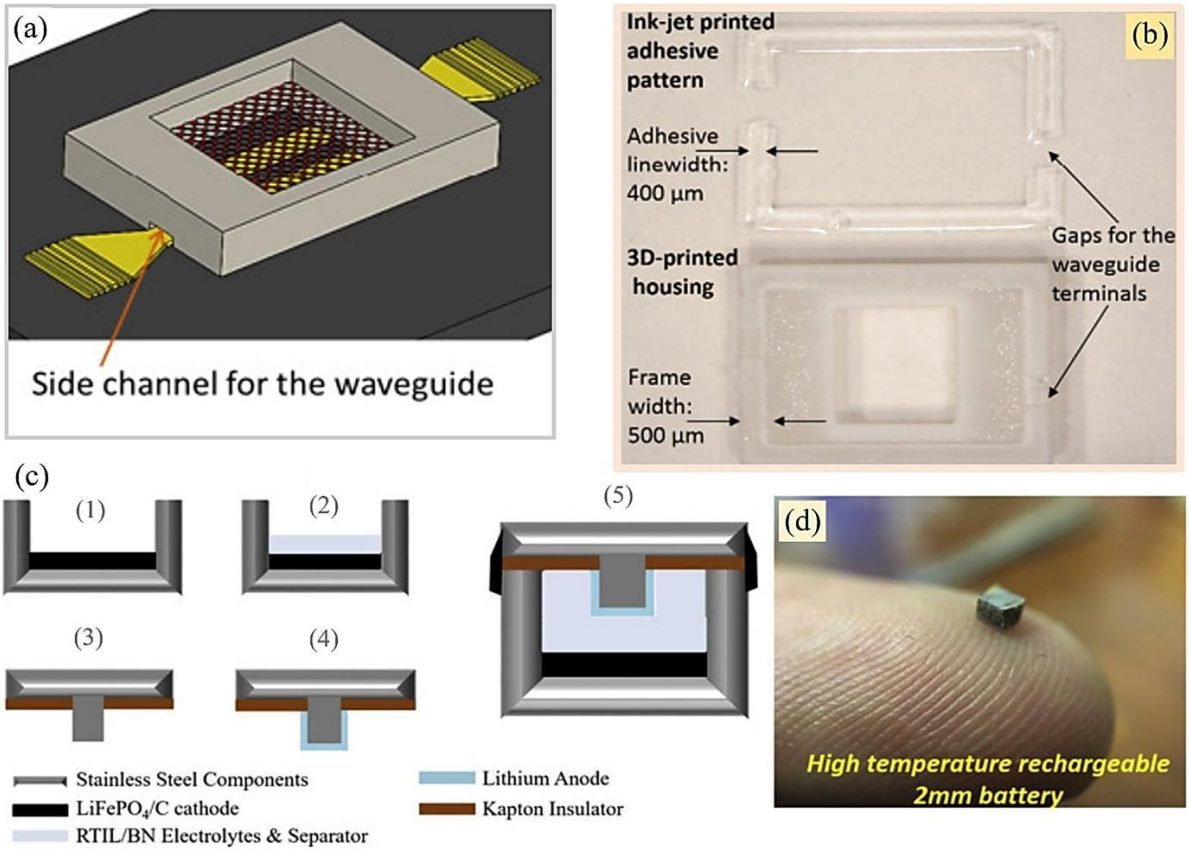

Figure 13: (a) Design of packaging with side channels. (b) An inkjet 3D printed package, Reproduced with permission [129] 2021, Elsevier (c) Assembly of packaged battery: (1) Cathode (stainless steel package) coated with spray ink; (2) adding the RTIL electrolyte and separator; (3) adding the Kapton insulator to the top and bottom lids; (4) adding the lithium anode on the top case projector; (5) the package sealed using urethane epoxy. (d) The fabricated lithium battery with the package, Reproduced with permission [130] 2021, Elsevier.

4.3. Microfluidics and Lap on a Chip Systems

Microfluidics is a group of microchannels that are used to handle fluids and reagents for biological and chemical applications such as disease diagnostics, culture cells and to examine chemical and biological processes [131]. Microfluidic systems are assembled from individual parts, allowing the flexibility to create complex microfluidic devices. Microfluidics are manufactured using either directly in one step or by replication. Direct processes are typically carried out using conventional subtractive or etching techniques such as micro machining, laser micromachining, micro electro discharge machining, injection moulding, focused ion beam, or photo lithography. Indirect or replication method is typically based on the soft lithographic methods [132]. Similarly, additive manufacturing was initially used to fabricate microfluidics indirectly using master moulds, which can be replicated using soft

lithography to create microfluidic devices. This reduces the need for the conventional microfabrication facilities as in cleanrooms [133]. The use of a 3D-printed master mould to fabricate microfluidics through soft lithography was the earliest approach to using additive manufacturing [134]. This was demonstrated by McDonald *et al*. in 2002 [134] using solid-object printing, which is similar to the multijet printing for fabricating the master mould and PDMS to obtain the replica microfluidic devices.

O'Connor et al. [135] employed inkjet printing to manufacture a master mould of a microfluidic pattern followed by soft lithography using PDMS. Rectangular microchannels with 260±10 µm in width and 350±100 µm in height were successfully fabricated. Heating and cooling micro channels were included in the design for the encapsulation of surfactant-free liver HepG2 cells using gelatin microgels. The microfluidic device was able to produce a droplet size of about 130 µm at 7.9 drops/second. The integrated heating and cooling channels efficiently controlled the temperature and prevented the droplets coalescence without surfactants. The HepG2 cell viability was 96.5% after two hours [135]. In another study, SLA was used to fabricate microfluidics master moulds, followed by a soft lithography process [136]. Generally, the surface roughness and the resolution of the fabricated microfluidics depend on the quality of the master mould. To improve the surface roughness, Villegas *et al*. [137] demonstrated a simple coating technique to enhance the surface quality of the additively manufactured mould by using fluorinated silane, which resulted in a smooth interface during the replica soft moulding. Using this approach, the microfluidic channels surface roughness (*Ra*) was improved from 2 µm to 0.2 µm, and it exhibited excellent optical properties and high resolution (Figure 14a to g). More complex master mould designs with internal and external features were assembled in a container and filled with PDMS pre-polymer to obtain flexible microfluidic parts [138]. A direct approach to rapidly manufacturing microfluidic devices using 3D printing in one step was also investigated by several researchers. Stereolithography approaches showed to hold a great promise to fabricate microfluidic systems for different applications, including biomedical, chemical, and soft robotics. An immunomagnetic flow microfluidic chip was fabricated by Lee et al. [139] using stereolithography. The fabricated cylinder's geometry was designed to reduce the flow velocity, which enabled handling of a high flow rate. The developed microfluidic device can handle 10 mL in 24 s, which is sufficient to process samples from 150 patients. A recent

study investigated using a two-photon stereolithography approach to 3D print complex microfluidic fully integrated system directly onto macroscale silica tubes. The authors mounted the silica tube onto the two-photon stereolithography printer which was placed in a photosensitive resin. This is followed by point-by-point scanning of the design using a focused femtosecond IR laser to initiate the crosslinking process of the microfluidic shape directly onto the tube. The results showed an effective sealing between the microfluidic and the tube, maintaining the fluid flow throughout the system channels and the outlets [140]. Digital light processing is capable of manufacturing negative Poisson's ratio materials. A honeycomb-based microfluidic device was fabricated using a hydrogel with negative Poisson's ratio to mimic vascular morphology and help to understand the movements of cancer cells inside the developed micro-channels [141]. On the other hand, two-photon lithography was used to manufacture microfluidic systems located at different heights with two crossed channels (Figure 14h and i) [142].

Fused deposition modelling (FDM) was employed to manufacture microfluidic systems for bacterial cultivation, PCR, and DNA isolation [143]. Anderson *et al* introduced the fabrication of a microfluidic device using inkjet printing for analysing cell viability and drug flow [144]. Recently, hydrogel micro-channels were also 3D printed using pneumatic material extrusion as replacements for blood vessels. Cell culture was achieved inside the developed micro-channels to investigate their biocompatibility. The cell viability was enhanced inside the micro-channels, which could potentially be used for cell survival, differentiation, and division [145].

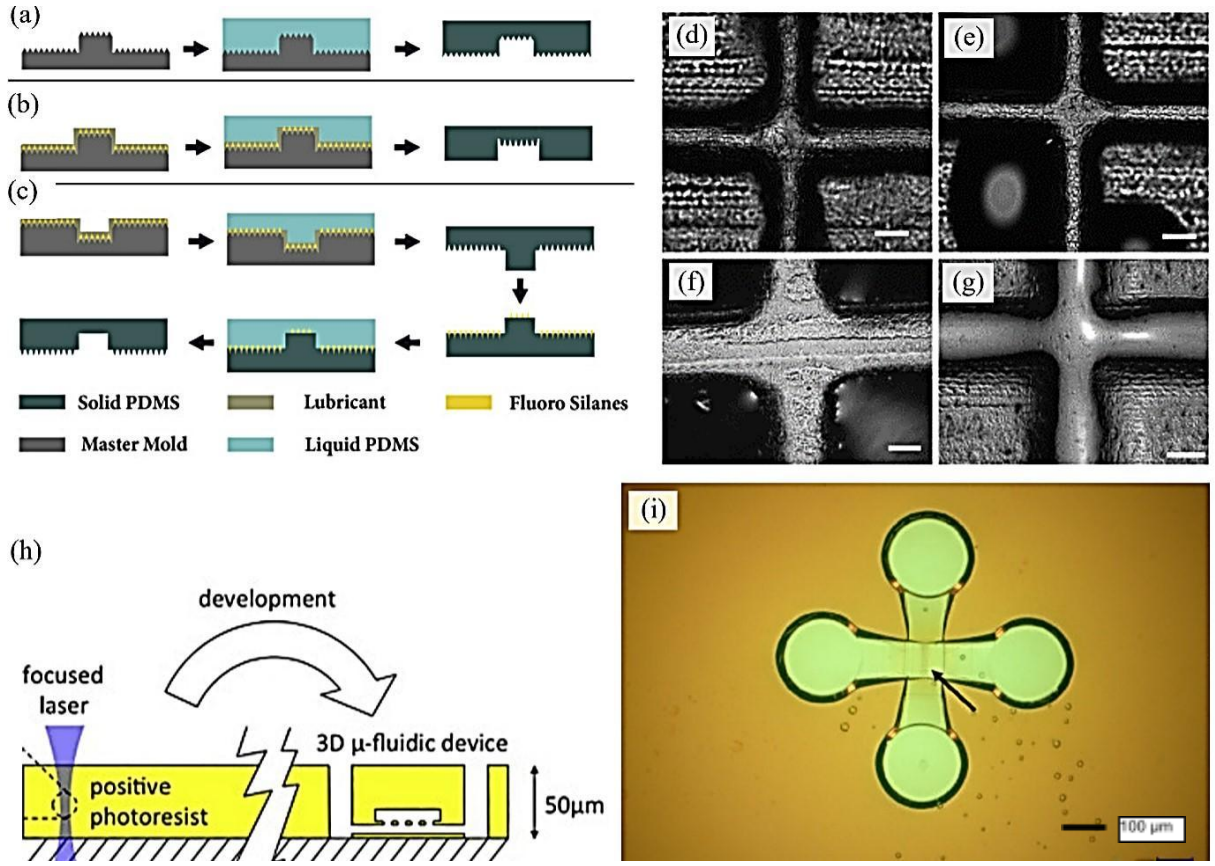

Figure 14: (a-c) A schematic diagram of microfluidics using 3D printing, coating, and soft lithography; (a) without coating to the 3D-printed master mould; (b) with a coated 3D-printed master mould; (c) with a coated PDMS soft mould. (d-g) PDMS microfluidic channels fabricated using (d) a master mould without coating; (e) a lubricated 3D-printed master mould; (f) a silanised coated master mould; (g) using a silanised PDMS mould, Reproduced with permission [137] 2021, Elsevier (h) A schematic diagram of the two-photon lithography process. (i) The fabricated microfluidic device with channels at different height levels, Reproduced with permission [142] 2021, Elsevier.

Lab-on-a-chip (LOC) is a tool used to develop small and user-friendly equipment to miniature the medicine, chemistry, and biotechnologies conventional laboratory equipment. Additively manufactured lab-on-chip devices are widely used to detect, diagnose, and biochemical analysis. The use of AM enabled the manufacturing of complex lab on chip systems at low cost and offered high chip density and enhanced volumetric efficiency [146].

Zhu et al. [147] produced a microfluidic lab on a chip system to trap and analyse zebrafish embryos using SLA and multijet printing. The optical properties of the 3D printed lab on a chip allowed performing angiogenesis assays. However, the materials used were toxic to zebrafish embryos. The authors managed to mitigate the toxicity of the printed materials

after soaking in ethanol for 24 hours [147]. Ma et al. [148] implemented DLP to 3D print liver lobule and vascular structures. Photopolymerised gelatin methacryloyl and glycidyl-methacrylated HA were used to encapsulate human induced stem cell-derived cardiomyocytes, endothelial and mesenchymal originated. The 3D printed lab on a chip showed a good performance in terms of better morphological organisation, gene expression, more significant metabolic secretion, and enhanced cytochrome induction. This enabled replicating the liver microenvironment and showed excellent potential for early personalised drug screening. Farazmand et al.[149] used SLA of transparent resin to fabricate a modular microfluidic and electrical integration lab on a prostate cancer diagnosis chip. The authors were able to achieve a volumetric flow rate of 33 ml/min without leakage by using a 3 µm wide release trench. The device also showed high sensitivity as the size was reduced.

Additive manufacturing has been used to manufacture a lab on a chip not only from a monolithic material but also multi-material were implemented to mimic the natural environment. Park et al. [150] developed an in house multi-nozzle material extrusion 3D printer to print a lab-on-chip system with airways and blood vessel networks to mimic the mucous in the human airway, which opens doors to perform preclinical drug trials [150]. Several advantages can be obtained using multi-materials 3D printing with versatile designs to replicate human tissue's [150]. However, there are still challenges to in vivo 3D print complex lab-on-chip devices to replace the natural environment. To overcome these issues, the design of lab-on-chip can be achieved by combining the microfluidic devices with a biomimetic 3D printed environment [151]. In addition, 4D printing of biomimetic systems can also be widely adopted to provide improved results for real-time monitoring of human cells or organs [152].

4.4. Structural MEMS

Additive manufacturing technologies have been demonstrated to fabricate MEMS using structural materials, including metals and ceramics, for the manufacture of micro thrusters, micro fuel cells, and micro turbines. Wei Liu *et al*. [86] investigated the use of microstereolithography to produce dense alumina and zirconia structural micro-components, which have the capability of working in harsh environments. The authors used ceramic powder mixed with photosensitive polymers to prepare a high solid loading

ceramic resin mix. Figure 15a shows the manufactured micro-components, which include micro-gears, periodic arrays, and micro-turbines [86]. A similar study was introduced to study the use of barium titanate [88], lead-free piezoceramics, and polymer derived ceramics [89]. The use of digital light processing was investigated to produce structural microparts made of polymer-based ceramic materials. Litrature is focused on the use of monolithic polymer-derived ceramics or mixed with ceramic fillers. Ceramics like silicon nitride, mullite, and SiOC micro-lattice parts were fabricated using DLP followed by high-temperature pyrolysis. Figure 15b and c show micro-lattices with a high resolution before and after sintering [153]. Touri *et al*. [79] demonstrated the capability of using pressure material extrusion to fabricate scaffolds using HA, phosphate powder, and calcium peroxide. The fabricated scaffold demonstrated a high porosity of 70% and a feature size of 400 µm, which is ideal for bone formation. The laser microsintering approach has become less favourable, and the research found in this area is limited. However, proof of concept to realise metal and ceramic parts using this approach is evident. Petsch *et al*. [105] employed laser microsintering techniques to fabricate metal and ceramic micro parts. The authors were able to process aluminium nitride and achieved high-density microparts. Alumina, SiC, SiO_x, and SiSiC have also been developed using laser microsintering [106, 107, 154]. Tungsten is difficult to process and was typically processed using micro-injection moulding to fabricate microparts for illumination applications. Ebert *et al*. [155] demonstrated the processing of Tungsten powder using micro-laser melting. They also investigated the effect of chamber pressure on the abrasion and density of the printed tungsten. Furthermore, a copper-based powder mix consisting of copper and copper- phosphorus alloy for 50W CW Nd:YAG laser microsintering has been explored, and both the densification and the process parameters have been investigated. The authors found that the liquid-phase sintering using copper-phosphorus alloy plays a key role in improving the densification of the microparts [156]. Hassanin *et al*. [157] introduced a hybrid additive manufacturing process to fabricated titanium microparts for biomedical applications, using powder bed fusion and micro-EDM to enhance resolution and surface roughness of the printed parts. The roughness *Ra* of the AM microparts was improved down to 0.7 µm. Ainsley *et al*. [158] used inkjet 3D printing to produce ceramic microparts with a thickness of 100 microns. The authors were able to control the droplet deposition by using an alkaline suspension to disperse the alumina particles. Freestanding

Microstructures and rotating wheels were successfully fabricated. Similarly, micro-maze structure of zirconia ceramic, with a thickness of about 170 µm was fabricated by Zhao *et al* [101]. Windsheimer *et al*. demonstrated the sheet lamination technique's use to fabricate ceramic micro-gears using thin sheets of silicon carbide preceramic Polymer [111]. The silicon carbide sheets were coated with a binder. Following 3D printing, the green components were heated in a furnace followed by silicon infiltration and pyrolysed at 1500 ℃ in vacuum to obtain Si-SiC microparts.

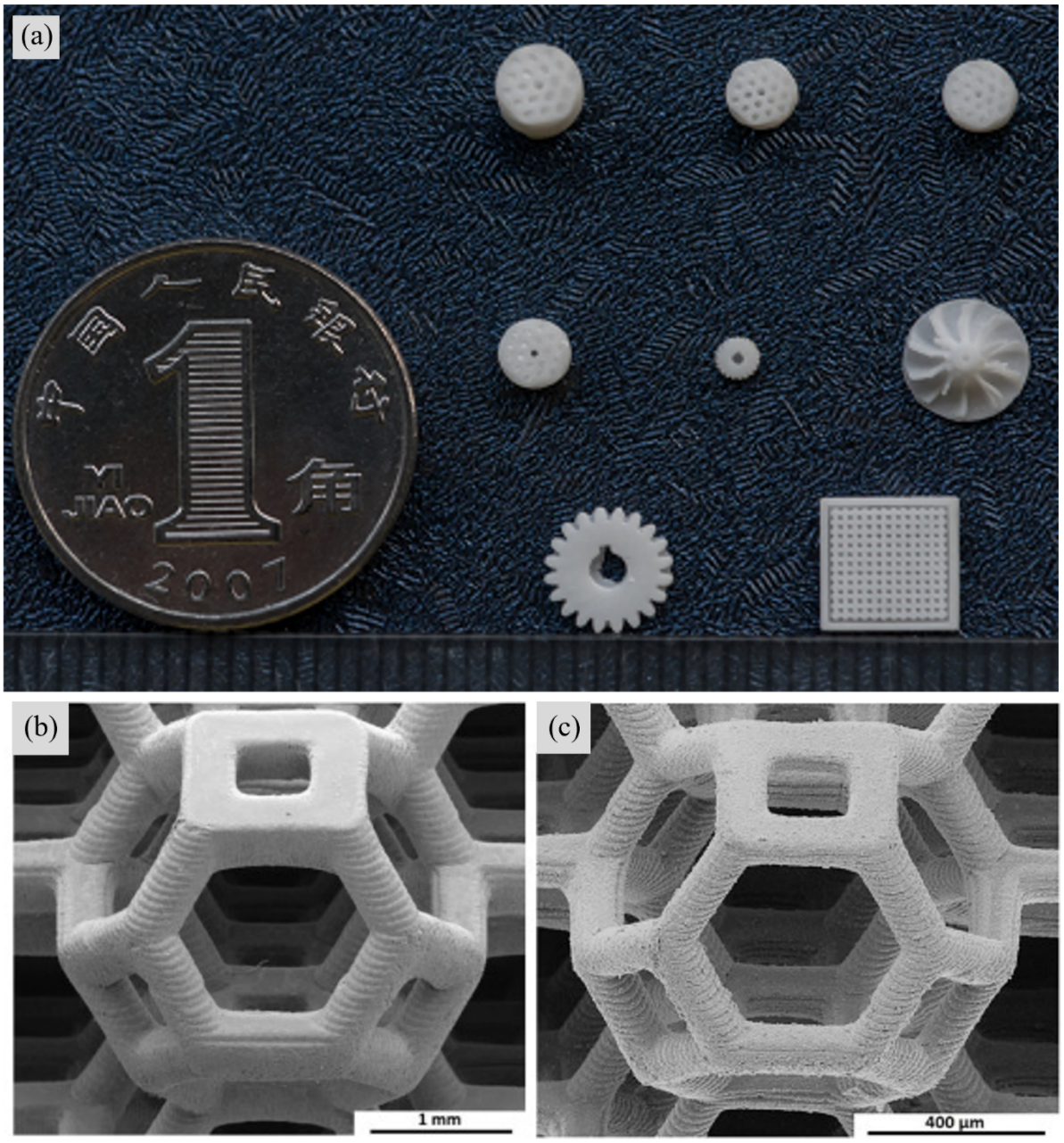

Figure 15: (a) Ceramic micro-parts manufactured using microstereolithography, Reproduced with permission [86] 2021, John Wiley & Sons, Inc (b) dried, and (c) pyrolysed samples fabricated using robocasting, Reproduced with permission [153] 2021, Elsevier.

5. Potential and Challenges

Conventional manufacturing approaches of MEMS are typically time-consuming and require cleanroom facilities to create 2D extruded structures using techniques such as photolithography or micromachining followed by a soft lithography process and bonding. A special glass mask may be required for every design to create a new master mould. Recently, Innovation in AM technologies has been significantly increased and led to the improvement of processes, resolution, ability to process more materials, understanding the interactions between processes and materials, and significant cost reduction of commercial 3D printers. The review shows that the integration of additive manufacturing into MEMS applications has been continuously becoming more popular. Initially, additive manufacturing was implemented for the manufacturing of micro-moulds for subsequent soft lithography or embossing processes. The use of additive manufacturing to create master moulds offers several benefits such as cost and time saving as the same master moulds can be used multiple times. Furthermore, the fabricated master moulds are compatible with many MEMS materials such as PDMS and silicon rubber. However, one limitation of using 3D-printed master moulds is that the geometric complexity is limited to the ability of the demoulding process [159].

As the technology evolved further in the past decade, directly-manufactured MEMS devices were demonstrated and have been mostly found to be successful from 2010 onwards. This shows the great economic, environmental and technical advantages of using AM over the traditional microfabrication methods. In fact, there are several advantages of AM in the MEMS industry, such as:

1. Personalisation and mass customisation.
2. On-demand and on-site fabrication.

3. Rapid design to manufacture and short lead-time.
4. The ability to manufacture complex geometries.
5. Materials savings and recycling.
6. Manufacturing of MEMS assemblies.
7. Improvement of the supply chain.
8. Improvement in products quality.
9. Manufacturing of lightweight MEMS.
10. Scalable production workflow.

With improvements in 3D printing technologies and their materials, microelectronics, microfluidics, lab on a chip, packages, and structural MEMS were directly 3D-printed in a single step. The literature reviewed in this paper showed excellent potentials for additive manufacturing as a promising tool in MEMS development. Six additive manufacturing technologies have been used to fabricate MEMS devices (Figure 16 and 17); these technologies are microstereolithography, material jetting, laser microsintering, laser-induced forward transfer, and sheet lamination. Figure 16 shows that microstereolithography and materials extrusion attracted the interest of many researchers and become more established for MEMS true 3D fabrication. This is because both techniques have advantages in processing many materials, fine resolution, and acceptable surface roughness. This is followed by materials jetting, laser-induced forward transfer, laser micro sintering, and which have found a great deal of interest from microelectronics and microfluidics researchers. On the other hand, research on using sheet lamination for microfabrication lacks because of the size limitation and poor surface roughness of this technique. Research connections between additive manufacturing (AM) technologies and different types of microelectromechanical systems are shown in Figure 17.

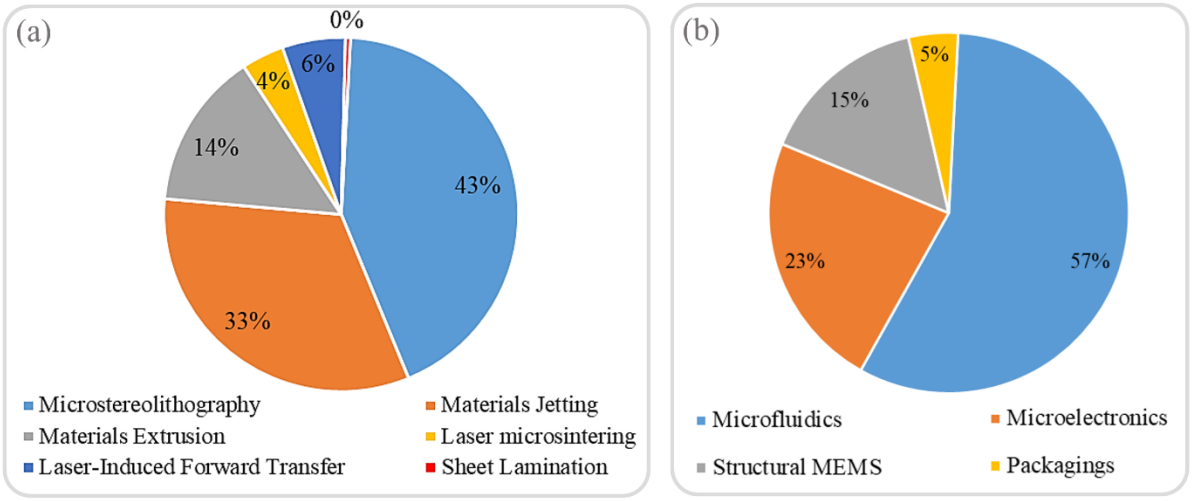

Figure 16: Quantity (in percentage) of publications on (a) AM techniques used in MEMS, and (b) MEMS categories processed using AM (Source: Scopus.com).

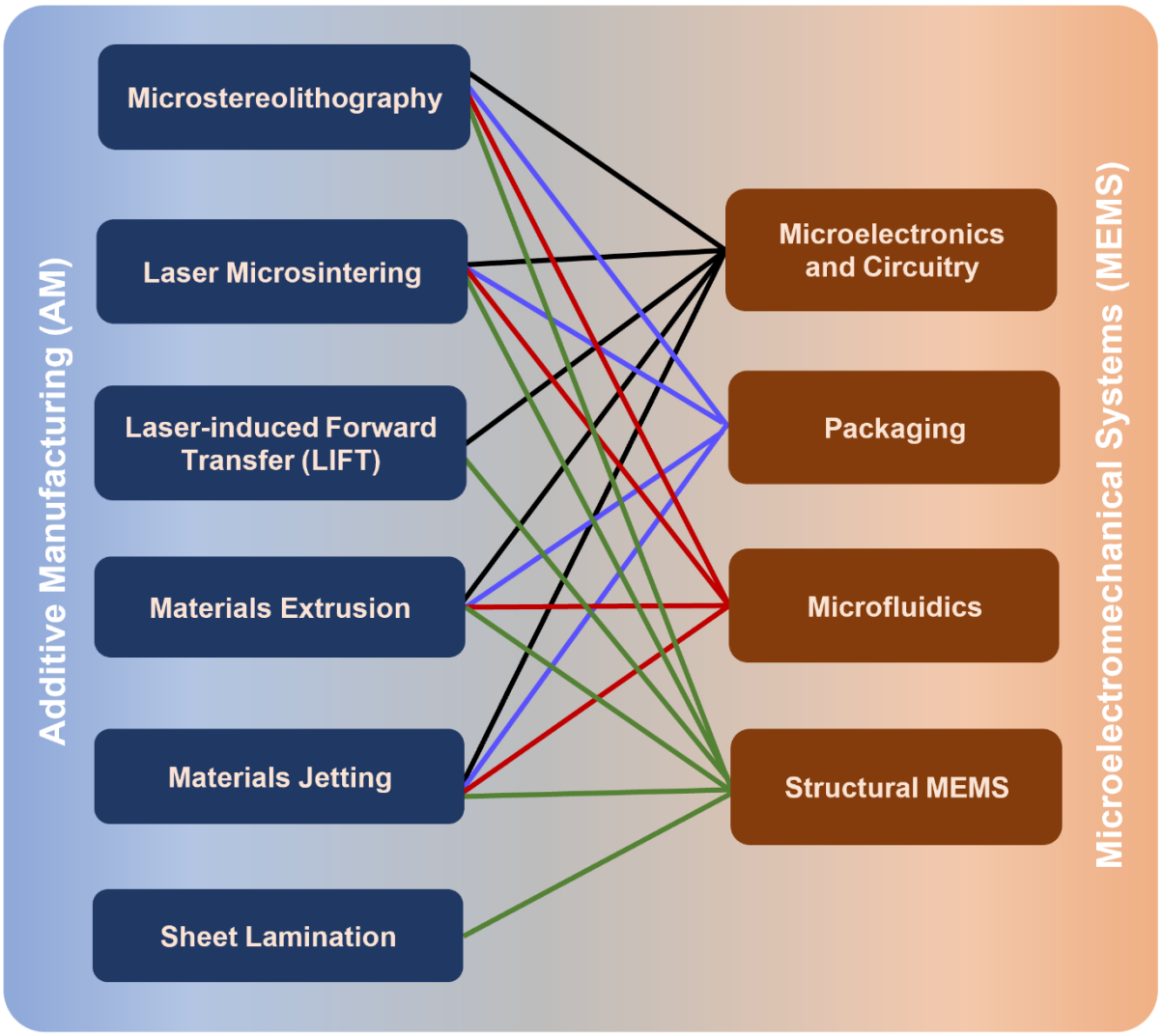

Figure 17: Research connections between additive manufacturing (AM) technologies and microelectromechanical systems (MEMS)

The state-of-the-art additive manufacturing technologies to develop MEMS applications offer promising alternatives to the exciting microfabrication processes and move rapidly from research-based concepts towards a longer-term adaption and commercialisation. Recent literature has shown that the current additive manufacturing of MEMS suffers from several challenges and limitations, constraining its wide usage within the MEMS community. This includes materials, geometric resolution, surface roughness, and productivity limitations.

Microstereolithography printed materials are typically stiff polymers. However, materials properties have been expanded to include materials with a wide range of flexibility such as silicone acrylates, similar to the PDMS properties [160]. This is in addition to high-performance polymers with high rigidity and other materials with up to 600 °C temperature resistance [77]. Although SLA processes offer a wide range of materials, including metal materials, achieving the full density of the final sintered parts is still challenging [161]. Optimisation of the resin suspension and sintering process could be one way to increase the achieved density. Detaching the structure from the building platform is one common issue of AM in general and SLA in particular. Levelling and cleaning of the building platform are techniques that can be used to improve the adhesion of the print to the building platform. Furthermore, 3D printing of hollow but closed parts is still an SLA problem as the uncured resin will trap inside the 3D printed parts. Controlling parts building direction can help in allowing the draining of the printed parts [162].

While the fused deposition modelling technology started the first wave of popularisation of additive manufacturing, it has not yet satisfied most of the MEMS requirements due to weaknesses such as poor surface roughness and low resolution. Fused deposition modelling exhibits poor mechanical properties due to the poor bonding between layers, defects and, porosity [163]. Alternatively, the building direction, layer thickness, and printing strategy affect the inherited poor surface quality. This is in addition to the stair-stepping effect of AM layers. The problems mentioned earlier are linked to fused deposition modelling and are common issues in all other additive manufacturing techniques; however, they are most significant in fused deposition modelling. Though post-processing steps are typically used to reduce the negative impact of these issues, they have not yet been explored for the additive manufacturing of MEMS. Laser Microsintering has difficulties that restrict its applications in MEMS industry. The inconsistent powder size and the developed heating affected zones are factors that deteriorate the resolution and the surface roughness of the 3D printed parts [13]. Equipment and process development are needed to overcome these challenges, such as introducing innovative powder recoating solutions and online artificial intelligence (AI) to monitor and optimise the process parameters. In Inkjet printing, challenges include the poor conductivity of the inks materials [83]. There are also limitations in the rheological requirements of the inks materials with specified operation viscosity and density ranges.

Therefore, the ink rheology, viscosity, solid loading, wetting characteristics, particle size and distribution, particle morphology, thermal properties, and substrate properties should be optimized during the preparation and processing of the ink. Similar to FDM, the resolution of the printing depends on the nozzle size [164]. The smaller the nozzle diameter, the higher resolution is the deposited ink. However, small nozzles are subjected to clogging and optimisation of the extrusion pressure, and the ink properties is the key to overcoming small nozzles issues [103].

There are still other issues, such as is the bonding of the 3D printed micro parts to the standard glass and silicon substrates. This is required to be addressed in-depth, and solutions to print MEMS into substrates directly are necessary to be developed. In addition, process simulation at the micro-level remains to be investigated to understand materials process interactions and the characterisation of different 3D-printed materials on various substrates.

6. Conclusions

This paper reviewed and evaluated both traditional and additive manufacturing technologies of MEMS and their applications. Techniques such as lithography, microinjection moulding, etching, laser micromachining, and microelectrical discharge machining are still attractive to the MEMS community. However, and over the past decade, additive manufacturing technologies of MEMS have significantly progressed, which has enabled their rapid 3D printing. The applications and potentials of AM technologies have been partly explored, but the results are promising. Microstereolithography, materials extrusion, and materials jetting have been widely investigated, while proof-of-concept studies were carried out for the use of sheet lamination and laser microsintering for fabricating truly 3D MEMS. A wide range of MEMS devices has been demonstrated using additive manufacturing, and various applications such as microelectronics, packaging, microfluidics, lab on a chip, and structural MEMS have shown great functional advancements, especially with the emerging of 4D printing, which allows more functionality of MEMS devices in the time domain. This paper showed that although additive manufacturing has contributed to the introduction of advanced true 3D MEMS, the technology still has to overcome several challenges. This includes inherited AM issues such as the need for post-processing, developing a high

performance and diverse range of materials, equipment innovation, surface quality, substrates adhesion, metrology and quality control, process modelling, and resolution.

References

1. W. Ahmed and K. Subraman: 'Emerging Nanotechnologies for Dentistry'; 2011, Oxford, William Andrew Publishing.
2. L. K. Prasad and H. Smyth, *Drug Development and Industrial Pharmacy*, 2016, **42**(7), 1019-1031.
3. K. Schwab: 'The Fourth Industrial Revolution: what it means, how to respond (2016)′', World Economic Forum, 2017.
4. C. Qiu, N. J. E. Adkins, H. Hassanin, M. M. Attallah, and K. Essa, *Materials & Design*, 2015, **87**, 845-853.
5. H. Klippstein, H. Hassanin, A. Diaz De Cerio Sanchez, Y. Zweiri, and L. Seneviratne, *Advanced Engineering Materials*, 2018, **20**(9), 1800290.
6. K. Essa, H. Hassanin, M. M. Attallah, N. J. Adkins, A. J. Musker, G. T. Roberts, N. Tenev, and M. Smith, *Applied Catalysis A: General*, 2017, **542**, 125-135.
7. S. Li, H. Hassanin, M. M. Attallah, N. J. E. Adkins, and K. Essa, *Acta Materialia*, 2016, **105**, 75-83.
8. H. Hassanin, L. Finet, S. C. Cox, P. Jamshidi, L. M. Grover, D. E. T. Shepherd, O. Addison, and M. M. Attallah, *Additive Manufacturing*, 2018, **20**, 144-155.
9. A. Sabouri, A. K. Yetisen, R. Sadigzade, H. Hassanin, K. Essa, and H. Butt, *Energy & Fuels*, 2017, **31**(3), 2524-2529.
10. H. Klippstein, A. Diaz De Cerio Sanchez, H. Hassanin, Y. Zweiri, and L. Seneviratne, *Advanced Engineering Materials*, 2018, **20**(2), 1700552.
11. A. Galatas, H. Hassanin, Y. Zweiri, and L. Seneviratne, *Polymers*, 2018, **10**(11), 1262.
12. K. S. Teh, *Frontiers of Mechanical Engineering*, 2017, **12**(4), 490-509.
13. M. Vaezi, H. Seitz, and S. Yang, *International Journal of Advanced Manufacturing Technology*, 2013, **67**(5-8), 1721-1754.
14. S. Arscott, *Lab on a Chip*, 2014, **14**(19), 3668-3689.
15. I. Zine-El-Abidine and M. Okoniewski, *IEEE Transactions on Advanced Packaging*, 2009, **32**(2), 448-452.
16. T. W. Harris: 'Chemical Milling'; 1976, Oxford, Clarendon Press.
17. K. Essa, F. Modica, M. Imbaby, M. A. El-Sayed, A. ElShaer, K. Jiang, and H. Hassanin, *The International Journal of Advanced Manufacturing Technology*, 2017, **91**(1), 445-452.
18. H. Hassanin and K. Jiang, *Journal of Micromechanics and Microengineering*, 2013, **24**(1), 015018.
19. H. Hassanin and K. Jiang, *Microelectronic Engineering*, 2011, **88**(11), 3275-3277.
20. H. Hassanin and K. Jiang, *Microelectronic Engineering*, 2010, **87**(5), 1610-1613.
21. H. Hassanin and K. Jiang, *Microelectronic Engineering*, 2009, **86**(4), 929-932.
22. H. Hassanin and K. Jiang, *Advanced Engineering Materials*, 2009, **11**(1‐2), 101-105.
23. H. Hassanin and K. Jiang, *Microelectronic Engineering*, 2010, **87**(5), 1617-1619.
24. S. Brittain, K. Paul, X.-M. Zhao, and G. Whitesides, *Physics World*, 1998, **11**(5), 31.
25. Y. Xia and G. M. Whitesides, *Annual Review of Materials Science*, 1998, **28**(1), 153-184.
26. J. A. Rogers and R. G. Nuzzo, *Materials Today*, 2005, **8**(2), 50-56.
27. M. Brehmer, L. Conrad, and L. Funk, *Journal of Dispersion Science and Technology*, 2003, **24**(3-4), 291-304.
28. J. H. Yoo and W. Gao, *International Journal of Modern Physics B*, 2003, **17**(8-9), 1147-1151.

29. P. Sarkar, O. Prakash, G. Wang, and R. Nicholson: 'Micro-laminate ceramic/ceramic composites (ysz/aizoq) by electrophoretic deposition′, 18th Annual Conference on Composites and Advanced Ceramic Materials, Cocoa Beach, 2009, John Wiley & Sons, 1019.
30. H. Von Both, M. Dauscher, and J. Haußelt: 'Fabrication of microstructured ceramics by electrophoretic deposition of optimized suspensions′, 28th International Conference on Advanced Ceramics and Composites Cocoa Beach, 2004, 135-140.
31. S. Bonnas, H.-J. Ritzhaupt-Kleissl, and J. Hausselt, *Journal of the European Ceramic Society*, 2010, **30**(5), 1159-1162.
32. J. Laubersheimer, H. J. Ritzhaupt-Kleissl, J. Hausselt, and G. Emig, *Journal of the European Ceramic Society*, 1998, **18**(3), 255-260.
33. S. Hill, *Materials World*, 2001, **9**(6), 24-25.
34. C. A. Griffiths, S. S. Dimov, E. B. Brousseau, and R. T. Hoyle, *Journal of Materials Processing Technology*, 2007, **189**(1-3), 418-427.
35. V. N. Stone, S. J. Baldock, L. A. Croasdell, L. A. Dillon, P. R. Fielden, N. J. Goddard, C. L. P. Thomas, and B. J. T. Brown, *Journal of Chromatography A*, 2007, **1155**(2), 199-205.
36. S. D. J. Hill, K. P. Kamper, U. Dasbach, J. Dopper, W. Erhfeld, and M. Kaupert: 'An investigation of computer modelling for micro-injection moulding′, Simulation and Design of Microsystems and Microstructures, Southampton, 1995, 275-283.
37. H. M. Chow, B. H. Yan, and F. Y. Huang, *Journal of Materials Processing Technology*, 1999, **91**(1), 161-166.
38. C. Shun-Tong, *Journal of Micromechanics and Microengineering*, 2008, **18**, 085002 (085009 pp.).
39. K. Egashira and K. Mizutani, *Precision Engineering*, 2002, **26**(3), 263-268.
40. F.-T. Weng, R. F. Shyu, and C.-S. Hsu, *Journal of Materials Processing Technology*, 2003, **140**, 332-334.
41. R. Phatthanakun, P. Songsiriritthigul, P. Klysubun, and N. Chomnawang: 'Multi-step powder casting and X-ray lithography of SU-8 resist for complicated 3D microstructures′, 5th International Conference on Electrical Engineering/Electronics, Computer, Telecommunications and Information Technology Piscataway, NJ, USA, 2008, IEEE, 805-808.
42. J. T. Sheu, K. S. You, C. H. Wu, and K. M. Chang: 'Optimization of KOH wet etching process in silicon nanofabrication′, Proceedings of the 2001 1st IEEE Conference on Nanotechnology. , Piscataway, NJ, USA, 2001, 213-217.
43. Y. F. Chang, Q. R. Chou, J. Y. Lin, and C. H. Lee, *Applied Physics A (Materials Science Processing)*, 2007, 193-196.
44. A. Sammak, S. Azimi, N. Izadi, B. K. Hosseinieh, and S. Mohajerzadeh, *Journal of Microelectromechanical Systems*, 2007, **16**(4), 912-918.
45. X. Y. Wei, Z. G. Zhu, P. D. Prewett, and K. Jiang, *Microelectronic Engineering*, 2007, **84**(5-8), 1256-1259.
46. H. M. a. S. Juodkazis: '3D Laser Microfabrication'; 2006, Weinheim, Germany, WILEY-VCH Verlag GmbH & Co.
47. C. Jimin and Y. Yuehua: 'Laser micro-fabrication in RF MEMS switches′, 2009 13th International Symposium on Antenna Technology and Applied Electromagnetics and the Canadian Radio Sciences Meeting, ANTEM/URSI 2009, February 15, 2009 - February 18, 2009, Banff, AB, Canada, 2009, Inst. of Elec. and Elec. Eng. Computer Society.

48. M. S. Amer, L. Dosser, S. LeClair, and J. F. Maguire, *Applied Surface Science*, 2002, **187**, 291-296.
49. M. S. Amer, M. A. El-Ashry, L. R. Dosser, K. E. Hix, J. F. Maguire, and B. Irwin, *Applied Surface Science*, 2005, **242**, 162-167.
50. B. E. Deal and A. Grove, *Journal of Applied Physics*, 1965, **36**(12), 3770-3778.
51. J. Nulman, J. Krusius, and A. Gat, *IEEE, Electron Device Letters*, 1985, **6**(5), 205-207.
52. M. J. Madou: 'Fundamentals of Microfabrication: The Science of Miniaturization'; 2002, Florida, CRC Press.
53. A. Dollet, *Surface and coatings Technology*, 2004, **177**, 245-251.
54. T. Haatainen, P. Majander, T. Makela, and J. Ahopelto: 'Imprinted 50 nm features by UV step and stamp imprint lithography method', 2007 Digest of papers Microprocesses and Nanotechnology, 5-8 Nov. 2007, 2007, 280-281.
55. Y. Yang and K. W. Leong: 'Chapter 1 - Microfluidic Cell Culture Platforms with Embedded Nanoscale Features', in 'Microfluidic Cell Culture Systems', (eds. C. Bettinger, et al.), 3-26; 2013, Oxford, William Andrew Publishing.
56. W. Ahmed, M. J. Jackson, and I. Ul Hassan: 'Chapter 1 - Nanotechnology to Nanomanufacturing', in 'Emerging Nanotechnologies for Manufacturing (Second Edition)', (eds. W. Ahmed, et al.), 1-13; 2015, Boston, William Andrew Publishing.
57. J.-S. Chu, M. D. Gilchrist, and N. Zhang: 'Microinjection Molding for Microfluidics Applications', in 'Encyclopedia of Microfluidics and Nanofluidics', (ed. D. Li), 2085-2101; 2015, New York, NY, Springer New York.
58. Z. Xiao, M. Dahmardeh, M. V. Moghaddam, A. Nojeh, and K. Takahata, *Microelectronic Engineering*, 2016, **150**, 64-70.
59. B. W. K. Woo, S. C. Gott, R. A. Peck, D. Yan, M. W. Rommelfanger, and M. P. Rao, *ACS applied materials & interfaces*, 2017, **9**(23), 20161-20168.
60. I. Litvinyuk and M. Rybachuk: 'Femtosecond laser micromachining of diamond: current research status, applications and challenges'; 2021,
61. Anon: 'Nanostructured Films and Coating by Evaporation, Sputtering, Thermal Spraying, Electro- and Electroles Deposition', in 'Handbook of Nanophase and Nanostructured Materials', (eds. Z. L. Wang, et al.), 246-277; 2002, Boston, MA, Springer US.
62. W. Ouyang and W. Wang, *Biomicrofluidics*, 2014, **8**(5), 052106.
63. V. Vasilyev, N. B. Morozova, T. Basova, I. Igumenov, and A. K. Hassan, *RSC Adv.*, 2015, **5**.
64. T. Langford, A. Mohammed, K. Essa, A. Elshaer, and H. Hassanin, *Applied Sciences*, 2021, **11**(1), 332.
65. M. A. El-Sayed, K. Essa, M. Ghazy, and H. Hassanin, *The International Journal of Advanced Manufacturing Technology*, 2020, **110**(9), 2257-2268.
66. H. Hassanin, A. Abena, M. A. Elsayed, and K. Essa, *Micromachines*, 2020, **11**(8), 745.
67. H. Hassanin, Y. Alkendi, M. Elsayed, K. Essa, and Y. Zweiri, *Advanced Engineering Materials*, 2020, **22**(3), 1901338.
68. X. Zhang, X. N. Jiang, and C. Sun, *Sensors and Actuators A: Physical*, 1999, **77**(2), 149-156.
69. Q. Geng, D. Wang, P. Chen, and S.-C. Chen, *Nature Communications*, 2019, **10**(1), 2179.
70. E. Behroodi, H. Latifi, and F. Najafi, *Scientific Reports*, 2019, **9**(1), 19692.

71. P. Regenfuss, A. Streek, L. Hartwig, S. Klötzer, T. Brabant, M. Horn, R. Ebert, and H. Exner, *Rapid Prototyping Journal*, 2007, **13**(4), 204-212.
72. N. K. Roy, D. Behera, O. G. Dibua, C. S. Foong, and M. A. Cullinan, *Microsystems & Nanoengineering*, 2019, **5**(1), 64.
73. R. Braudy, *Proceedings of the IEEE*, 1969, **57**(10), 1771-1772.
74. J. Bohandy, B. Kim, and F. Adrian, *Journal of Applied Physics*, 1986, **60**(4), 1538-1539.
75. A. Piqué, R. C. Y. Auyeung, H. Kim, N. Charipar, and S. Mathews, *Journal of Physics D: Applied Physics*, 2016, **49**, 223001.
76. R. Bähnisch, W. Groß, J. Staud, and A. Menschig, *Sensors and Actuators A: Physical*, 1999, **74**(1), 31-34.
77. T. D. Ngo, A. Kashani, G. Imbalzano, K. T. Q. Nguyen, and D. Hui, *Composites Part B: Engineering*, 2018, **143**, 172-196.
78. K. Cai, B. Román-Manso, J. E. Smay, J. Zhou, M. I. Osendi, M. Belmonte, and P. Miranzo, *Journal of the American Ceramic Society*, 2012, **95**(8), 2660-2666.
79. M. Touri, F. Moztarzadeh, N. A. A. Osman, M. M. Dehghan, and M. Mozafari, *Ceramics International*, 2019, **45**(1), 805-816.
80. I. Endo, S. Ohno, Y. Sato, S. Saito, and T. Nakagiri, *Liquid jet recording process and apparatus therefor*. 1982, Google Patents.
81. J. Brünahl and A. M. Grishin, *Sensors and Actuators A: Physical*, 2002, **101**(3), 371-382.
82. A. Shama: 'Study of Microfluidic Mixing and Droplet Generation for 3D Printing of Nuclear Fuels', 2017.
83. A. Roshanghias, M. Dreissigacker, C. Scherf, C. Bretthauer, L. Rauter, J. Zikulnig, T. Braun, K. F. Becker, S. Rzepka, and M. Schneider-Ramelow, *Micromachines*, 2020, **11**(6).
84. D. X. Luong, A. K. Subramanian, G. A. L. Silva, J. Yoon, S. Cofer, K. Yang, P. S. Owuor, T. Wang, Z. Wang, J. Lou, P. M. Ajayan, and J. M. Tour, *Advanced Materials*, 2018, **30**(28), 1707416.
85. G. T. Chu, G. A. Brady, W. Miao, and J. W. Halloran, *MRS Proceedings*, 1998, **542**, 119.
86. W. Liu, H. Wu, Z. Tian, Y. Li, Z. Zhao, M. Huang, X. Deng, Z. Xie, and S. Wu, *Journal of the American Ceramic Society*, 2019, **102**(5), 2257-2262.
87. V. K. Varadan and V. V. Varadan: 'Micro stereo lithography for fabrication of 3D polymeric and ceramic MEMS′, Proceedings of SPIE - The International Society for Optical Engineering, 2001, 147-157.
88. X. Song, Z. Chen, L. Lei, K. Shung, Q. Zhou, and Y. Chen, *Rapid Prototyping Journal*, 2017, **23**(1), 44-53.
89. W. Chen, F. Wang, K. Yan, Y. Zhang, and D. Wu, *Ceramics International*, 2019, **45**(4), 4880-4885.
90. Z. C. Eckel, C. Zhou, J. H. Martin, A. J. Jacobsen, W. B. Carter, and T. A. Schaedler, *Science*, 2016, **351**(6268), 58-62.
91. X. Zheng, H. Lee, T. Weisgraber, M. Shusteff, J. DeOtte, E. Duoss, J. Kuntz, M. Biener, Q. Ge, J. Jackson, S. Kucheyev, N. Fang, and C. Spadaccini, *Science*, 2014, **344**, 1373-1377.
92. Y.-M. Ha, J.-W. Choi, and S. Lee, *Journal of Mechanical Science and Technology*, 2008, **22**, 514-521.
93. E. Käpylä, S. Turunen, and M. Kellomäki, *Micro and Nanosystems*, 2010, **2**(2), 87-99.

94. X. Zhou, Y. Hou, and J. Lin, *AIP Advances*, 2015, **5**(3), 030701.
95. K.-S. Lee, R. H. Kim, D.-Y. Yang, and S. H. Park, *Progress in Polymer Science*, 2008, **33**(6), 631-681.
96. H. O. T. Ware and C. Sun, *Journal of Micro and Nano-Manufacturing*, 2019, **7**(3).
97. J. Bauer, C. Crook, A. Guell Izard, Z. C. Eckel, N. Ruvalcaba, T. A. Schaedler, and L. Valdevit, *Matter*, 2019, **1**(6), 1547-1556.
98. J. R. Tumbleston, D. Shirvanyants, N. Ermoshkin, R. Janusziewicz, A. R. Johnson, D. Kelly, K. Chen, R. Pinschmidt, J. P. Rolland, A. Ermoshkin, E. T. Samulski, and J. M. DeSimone, *Science*, 2015, **347**(6228), 1349-1352.
99. W. Huang, X. Zhang, Q. Wu, and B. Wu, *Rapid Prototyping Journal*, 2013, **19**(5), 319-326.
100. E. Peng, D. Zhang, and J. Ding, *Advanced Materials*, 2018, **30**(47), 1802404.
101. X. Zhao†, J. R. G. Evans, M. J. Edirisinghe, and J.-H. Song, *Journal of the American Ceramic Society*, 2002, **85**(8), 2113-2115.
102. J. Lessing, A. C. Glavan, S. B. Walker, C. Keplinger, J. A. Lewis, and G. M. Whitesides, *Advanced Materials*, 2014, **26**(27), 4677-4682.
103. M. A. Skylar-Scott, S. Gunasekaran, and J. A. Lewis, *Proceedings of the National Academy of Sciences*, 2016, **113**(22), 6137-6142.
104. P. Regenfuss, *Rapid Prototyping Journal*, 2007, **13**(4), 204-212.
105. T. Petsch, P. Regenfuß, R. Ebert, L. Hartwig, S. Klötzer, T. Brabant, and H. Exner: 'Industrial laser micro sintering', ICALEO 2004 - 23rd International Congress on Applications of Laser and Electro-Optics, Congress Proceedings, 2004.
106. J. Chen, J. Yang, and T. Zuo: 'Micro Fabrication with Selective Laser Micro Sintering', 2006 1st IEEE International Conference on Nano/Micro Engineered and Molecular Systems, 18-21 Jan. 2006, 2006, 426-429.
107. H. Exner, M. Horn, A. Streek, F. Ullmann, L. Hartwig, P. Regenfuß, and R. Ebert, *Virtual and Physical Prototyping*, 2008, **3**(1), 3-11.
108. D. Chrisey, A. Pique, J. Fitz-Gerald, R. C. Y. Auyeung, R. McGill, H. D. Wu, and M. Duignan, *Ž . Applied Surface Science*, 2000, **154155**, 593-600.
109. C. W. Visser, R. Pohl, C. Sun, G.-W. Römer, B. Huis in 't Veld, and D. Lohse, *Advanced Materials*, 2015, **27**(27), 4087-4092.
110. A. Piqué, D. Chrisey, R. C. Y. Auyeung, J. Fitz-Gerald, H. D. Wu, R. McGill, S. Lakeou, P. K. Wu, V. Nguyen, and M. Duignan, *Applied Physics A*, 1999, **69**, S279-S284.
111. H. Windsheimer, N. Travitzky, A. Hofenauer, and P. Greil, *Advanced Materials*, 2007, **19**(24), 4515-4519.
112. C. J. Robinson, B. Stucker, A. J. Lopes, R. Wicker, and J. A. Palmer, *17th Solid Freeform Fabrication Symposium, SFF 2006*, 2006, 60-69.
113. J. J. Adams, E. B. Duoss, T. F. Malkowski, M. J. Motala, B. Y. Ahn, R. G. Nuzzo, J. T. Bernhard, and J. A. Lewis, *Advanced Materials*, 2011, **23**(11), 1335-1340.
114. N. Zhou, C. Liu, J. A. Lewis, and D. Ham, *Advanced Materials*, 2017, **29**(15), 1605198.
115. C. Liu, X. Cheng, B. Li, Z. Chen, S. Mi, and C. Lao, *Materials (Basel, Switzerland)*, 2017, **10**(8).
116. S. Castillo, D. Muse, F. Medina, E. MacDonald, and R. Wicker: 'Electronics integration in conformal substrates fabricated with additive layered manufacturing', 20th Annual International Solid Freeform Fabrication Symposium, SFF 2009, 2009, 730-737.

117. G. D. Liu, C. H. Wang, Z. L. Jia, and K. X. Wang, *Journal of Micromechanics and Microengineering*, 2021, **31**(6).
118. J. Odent, T. J. Wallin, W. Pan, K. Kruemplestaedter, R. F. Shepherd, and E. P. Giannelis, *Advanced Functional Materials*, 2017, **27**(33), 1701807.
119. Q. Mu, L. Wang, C. K. Dunn, X. Kuang, F. Duan, Z. Zhang, H. J. Qi, and T. Wang, *Additive Manufacturing*, 2017, **18**, 74-83.
120. S. Ghoshal, *Fibers*, 2017, **5**(4), 40.
121. D. S. Kolchanov, I. Mitrofanov, A. Kim, Y. Koshtyal, A. Rumyantsev, E. Sergeeva, A. Vinogradov, A. Popovich, and M. Y. Maximov, *Energy Technology*, 2020, **8**(3), 1901086.
122. H. Esrom, J.-Y. Zhang, U. Kogelschatz, and A. J. Pedraza, *Applied Surface Science*, 1995, **86**(1), 202-207.
123. T. H. J. van Osch, J. Perelaer, A. W. M. de Laat, and U. S. Schubert, *Advanced Materials*, 2008, **20**(2), 343-345.
124. S.-Y. Wu, C. Yang, W. Hsu, and L. Lin, *Microsystems & Nanoengineering*, 2015, **1**(1), 15013.
125. J. Hörber, C. Goth, and J. Franke, *International Symposium on Microelectronics*, 2012, **2012**, 000741-000748.
126. G. Aspar, B. Goubault, O. Lebaigue, J. C. Souriau, G. Simon, L. D. Cioccio, and Y. Brechet: '3D Printing as a New Packaging Approach for MEMS and Electronic Devices′, Proceedings - Electronic Components and Technology Conference, 2017, 1071-1079.
127. B. Goubault, G. Aspar, J. C. Souriau, L. Castagne, S. Simon, L. Di Cioccio, and Y. Brechet: 'A New Microsystem Packaging Approach Using 3D Printing Encapsulation Process′, Proceedings - Electronic Components and Technology Conference, 2018, 118-124.
128. B. Tehrani, R. A. Bahr, W. Su, B. Cook, and M. Tentzeris: 'E-band characterization of 3D-printed dielectrics for fully-printed millimeter-wave wireless system packaging', 1756-1759; 2017,
129. Y. Ma, J. Kaczynski, C. Ranacher, A. Roshanghias, M. Zauner, and B. Abasahl, *Microelectronic Engineering*, 2018, **198**, 29-34.
130. N. Masurkar, G. Babu, S. Porchelvan, and L. M. Reddy Arava, *Journal of Power Sources*, 2018, **399**, 179-185.
131. W. Lee, D. Kwon, W. Choi, G. Y. Jung, A. K. Au, A. Folch, and S. Jeon, *Scientific Reports*, 2015, **5**(1), 7717.
132. S. M. Scott and Z. Ali, *Micromachines*, 2021, **12**(3), 319.
133. A. Waldbaur, H. Rapp, K. Länge, and B. E. Rapp, *Analytical Methods*, 2011, **3**(12), 2681-2716.
134. J. C. McDonald, M. L. Chabinyc, S. J. Metallo, J. R. Anderson, A. D. Stroock, and G. M. Whitesides, *Analytical Chemistry*, 2002, **74**(7), 1537-1545.
135. J. S. O'Connor, H. Kim, E. Gwag, L. Abelmann, B. Sung, and A. Manz: '3D Printing for Microgel-Based Liver Cell Encapsulation′, Proceedings of the IEEE International Conference on Micro Electro Mechanical Systems (MEMS), 2021, 1023-1026.
136. G. Comina, A. Suska, and D. Filippini, *Lab on a Chip*, 2014, **14**(16), 2978-2982.
137. M. Villegas, Z. Cetinic, A. Shakeri, and T. F. Didar, *Analytica Chimica Acta*, 2018, **1000**, 248-255.
138. H. N. Chan, Y. Chen, Y. Shu, Y. Chen, Q. Tian, and H. Wu, *Microfluidics and Nanofluidics*, 2015, **19**(1), 9-18.

139. W. Lee, D. Kwon, B. Chung, G. Y. Jung, A. Au, A. Folch, and S. Jeon, *Anal Chem*, 2014, **86**(13), 6683-6688.
140. R. Acevedo, Z. Wen, I. B. Rosenthal, E. Z. Freeman, M. Restaino, N. Gonzalez, and R. D. Sochol: '3d Nanoprinted External Microfluidic Structures Via Ex Situ Direct Laser Writing', Proceedings of the IEEE International Conference on Micro Electro Mechanical Systems (MEMS), 2021, 10-13.
141. D. Y. Fozdar, P. Soman, J. W. Lee, L. H. Han, and S. Chen, *Adv Funct Mater*, 2011, **21**(14), 2712-2720.
142. G. van der Velden, D. Fan, and U. Staufer, *Micro and Nano Engineering*, 2020, **7**, 100054.
143. D. Chudobova, K. Cihalova, S. Skalickova, J. Zitka, M. A. Rodrigo, V. Milosavljevic, D. Hynek, P. Kopel, R. Vesely, V. Adam, and R. Kizek, *Electrophoresis*, 2015, **36**(3), 457-466.
144. K. B. Anderson, S. Y. Lockwood, R. S. Martin, and D. M. Spence, *Anal Chem*, 2013, **85**(12), 5622-5626.
145. L. E. Bertassoni, M. Cecconi, V. Manoharan, M. Nikkhah, J. Hjortnaes, A. L. Cristino, G. Barabaschi, D. Demarchi, M. R. Dokmeci, Y. Yang, and A. Khademhosseini, *Lab on a Chip*, 2014, **14**(13), 2202-2211.
146. M. Carve and D. Wlodkowic, *Micromachines*, 2018, **9**(2), 91.
147. F. Zhu, N. Macdonald, J. Cooper, and D. Wlodkowic: 'Additive manufacturing of lab-on-a-chip devices: promises and challenges'; 2013, SPIE.
148. X. Ma, X. Qu, W. Zhu, Y.-S. Li, S. Yuan, H. Zhang, J. Liu, P. Wang, C. S. E. Lai, F. Zanella, G.-S. Feng, F. Sheikh, S. Chien, and S. Chen, *Proceedings of the National Academy of Sciences*, 2016, **113**(8), 2206-2211.
149. M. H. Farazmand, R. Rodrigues, J. W. Gardner, and J. Charmet: 'Design and Development of a Disposable Lab-on-a-Chip for Prostate Cancer Detection', 2019 41st Annual International Conference of the IEEE Engineering in Medicine and Biology Society (EMBC), 23-27 July 2019, 2019, 1579-1583.
150. J. Y. Park, H. Ryu, B. Lee, D.-H. Ha, M. Ahn, S. Kim, J. Y. Kim, N. L. Jeon, and D.-W. Cho, *Biofabrication*, 2018, **11**(1), 015002.
151. J. Sapudom and T. Pompe, *Biomaterials Science*, 2018, **6**(8), 2009-2024.
152. A. Sydney Gladman, E. A. Matsumoto, R. G. Nuzzo, L. Mahadevan, and J. A. Lewis, *Nature Materials*, 2016, **15**(4), 413-418.
153. J. Schmidt and P. Colombo, *Journal of the European Ceramic Society*, 2018, **38**(1), 57-66.
154. A. Streek, P. Regenfuß, T. Süß, R. Ebert, and H. Exner: 'Laser micro sintering of SiO2 with an NIR-laser'; 2008, SPIE.
155. R. Ebert, F. Ullmann, L. Hartwig, T. Suess, S. Kloetzer, A. Streek, J. Schille, P. Regenfuss, and H. Exner: 'Laser microsintering of tungsten in vacuum', Proceedings of SPIE - The International Society for Optical Engineering, 2010.
156. C. Dai, H. H. Zhu, L. D. Ke, W. J. Lei, and B. J. Chen: 'Development a Cu-based metal powder for selective laser micro sintering', 1 Journal of Physics: Conference Series, 2011.
157. H. Hassanin, F. Modica, M. A. El-Sayed, J. Liu, and K. Essa, *Advanced Engineering Materials*, 2016, **18**(9), 1544-1549.
158. B. Derby, *Journal of Materials Science*, 2002, **37**, 3091-3092.
159. M. S. Thomas, B. Millare, J. M. Clift, D. Bao, C. Hong, and V. I. Vullev, *Annals of Biomedical Engineering*, 2010, **38**(1), 21-32.

160. N. Bhattacharjee, C. Parra-Cabrera, Y. T. Kim, A. P. Kuo, and A. Folch, *Advanced Materials*, 2018, **30**(22), 1800001.
161. E. Fantino, A. Chiappone, I. Roppolo, D. Manfredi, R. Bongiovanni, C. F. Pirri, and F. Calignano, *Advanced Materials*, 2016, **28**(19), 3712-3717.
162. Y. Pan, H. He, J. Xu, and A. Feinerman, *Rapid Prototyping Journal*, 2017, **23**(2), 353-361.
163. A. Licciulli, C. E. Corcione, A. Greco, V. Amicarelli, and A. Maffezzoli, *Journal of The European Ceramic Society*, 2005, **25**(9), 1581-1589.
164. J. A. Lewis, *Advanced Functional Materials*, 2006, **16**(17), 2193-2204.